ISSN 1407-5806

COMPUTER MODELLING AND NEW TECHNOLOGIES

Volume 8
No 1

2004

Transporta un sakaru institūts
(Transport and Telecommunication Institute)

Computer Modelling and New Technologies

Volume 8, No.1 – 2004

ISSN 1407-5806
ISSN 1407-5814
(On-line: www.tsi.lv)

Riga – 2004

THE JOURNAL IS DESIGNED FOR PUBLISHING PAPERS CONCERNING THE FOLLOWING FIELDS OF RESEARCH:

- mathematical and computer modelling
- mathematical methods in natural and engineering sciences
- physical and technical sciences
- computer sciences and technologies
- semiconductor electronics and semiconductor technologies
- aviation and aerospace technologies
- electronics and telecommunication
- navigation and radar systems
- telematics and information technologies
- transport and logistics
- economics and management
- social sciences

Articles can be presented in journal in English (preferably), Russian, German and Latvian (at the option of authors). All articles are reviewed.

EDITORIAL CORRESPONDENCE
Transporta un sakaru institūts (Transport and Telecommunication Institute)
Lomonosova iela 1, LV-1019, Riga, Latvia. Phone: (+371)-7100593. Fax: (+371)-7100535.
E-mail: journal@tsi.lv, http:// www.tsi.lv

COMPUTER MODELLING AND NEW TECHNOLOGIES, 2004, Vol. 8, No.1
ISSN 1407-5806, **ISSN** 1407-5814 (on-line: www.tsi.lv)
Scientific and research journal of Transport and Telecommunication Institute (Riga, Latvia)
The journal is being published since 1996.

CONTENTS

Editors' Remarks

To the Heavens above us
O look and behold
The Planets that love us
All harnessed in gold!
What chariots, what horses
Against us shall bide
While the Stars in their courses
Do fight on our side?

All thought, all desires,
That are under the sun,
Are one with their fires,
As we also are one:
All matter, all spirit,
All fashion, all frame,
Receive and inherit
Their strength from the same.

(Oh, man that deniest
All power save thine own,
Their power in the highest
Is mightily shown.
Not less in the lowest
That power is made clear.
Oh, man, if thou knowest,
What treasure is here!)

****

From: An Astrologer's Song ***Rudyard Kipling***[1] (1865-1936)

This 8th volume continues our publishing policy. The new format of journal (4 No per year) allows us to present new scientific results of contributors in a shorter time. This also means that evidently we divide the main topics of the journal into different issues.

The present issue is the continuation of our publishing activities. We hope our journal will be interesting for research community, and we are open for collaboration both in research and publishing.

EDITORS

Yu. N. Shunin

I.V. Kabashkin

[1] **Rudyard Kipling (1865-1936)** was born in India at the time of the British Empire. His father was the Headmaster of a school in Bombay, and Kipling was sent at age six to a boarding school in England. He returned to India in 1882, and began work as a journalist on the 'Civil and Military' Gazette, while quickly gaining a reputation as a great writer. Kipling stands as a literary giant with a whole host of classic books to his name such as *Kim*, and *The Jungle Book.* Of his many poems his most famous is probably *'If'* which even today the encapsulation of a mini-degree course is in human psychology. He received the Nobel Prize for literature in 1907, and when he died was buried in Poet's corner at Westminster Abbey.

Computer Modelling & New Technologies, 2004, Volume 8, No.1, 7-19
Transport and Telecommunication Institute, Lomonosov Str.1, Riga, LV-1019, Latvia

MODELLING OF PATTERN FORMATION IN THIN METALLIC FILM GROWTH ON CRYSTALLINE SUBSTRATES

V.N.KUZOVKOV, E.A. KOTOMIN, G. ZVEJNIEKS

Institute for Solid State Physics, University of Latvia, Kengaraga 8, LV-1063 Riga, Latvia

We present and discuss results of the kinetic MC simulations of the pattern formation during the adsorption of mobile metal atoms on crystalline substrate. Simulations are based on a new complete axiomatic approach to the kinetics of diffusion-controlled processes with energetic interactions (the *standard model* described in Appendix A). Pattern formation simulated for submonolayer metal coverage is characterized in terms of the joint correlation functions for spatial distribution of adsorbed atoms. We demonstrate that the patterns obtained are defined by the ratio of the atom mutual attraction energy to the substrate temperature. Kinetic MC simulations confirm the distinctive average distance between two-dimensional metal islands, estimated by means of scaling approach.
Keywords: *pattern formation, thin films, MC simulations*

1. Introduction

Metal atoms adsorption with a given dose rate on metallic and insulating substrates shows in general two modes of thin film growth: monolayer-by-monolayer regime or $\boldsymbol{D}$=3 ($\boldsymbol{D}$ – spatial dimensionality) metal cluster formation [1-4]. Detailed understanding of this process is important for many technological applications, including catalysis, microelectronics etc. In particular, the problem of Ag thin film deposition on MgO is widely studied [5-7]. Electron microscopy experiments performed at low and moderate temperatures reveal two kinds of *pattern formation*: the spherical compact clusters and worm-like loose cluster growth [7,8]. The analysis of these structures reveals some regularity. At the constant temperature the change of adsorbate concentration increases the size of metallic clusters, but the characteristic distance between cluster centres remains almost unchanged, being of the order 0.1 μm, i.e., a few hundreds of lattice constants. The more so, wide variations of Ag adsorption rate and the temperature do not affect strongly this characteristic distance. However, the temperature increase from 100 C up to 450 C transforms loose clusters into compact ones [7].

There are two kinds of general approaches in theoretical description of the growth mode of thin metallic films. The first approach assumes the system to be in a thermo dynamical equilibrium and thus the statistical methods could be applied [9,10]. In fact, constant adsorbate concentration is assumed, i.e. the adsorption rate is expected to be very slow whereas metal atom diffusion very fast, so that the system reaches the thermodynamic equilibrium between adsorption of the two sequential metal atoms. This is not, however, the case when adsorbate atoms strongly interact with each other, which prevents a fast transformation of small clusters into larger clusters (Ostwald ripening).

The alternative *kinetic* approach, which is usually based on rate-equations, focuses on the mobile atom diffusion and aggregation [3]. Often the relaxation kinetics is modelled by means of Monte Carlo (MC) or similar techniques for systems with a constant number of particles where Ostwald ripening occurs [11,12]. We would like to mention in this respect pioneering papers by Ben-Shaul *et al* [13,14] where pattern formation was studied as a result of a strong adsorbate-adsorbate interaction and diffusion.

Most of the kinetic MC simulations (see, e.g., [15-17] and references therein) deal with irreversible growth of aggregates, which corresponds to the limiting case of very strong adsorbate-adsorbate interaction and/or low temperatures. This leads typically to the dendrite-like adsorbate patterns. Rare exceptions are the kinetic MC simulations [18,19] where adatoms attachment to islands is a reversible process.

In this paper, we perform MC simulations for a realistic process of adsorbate deposition with a given rate, taking into account adsorbate surface diffusion and interaction. To describe the spatial distribution of adsorbed atoms, we use for the first time the joint correlation functions characterizing relative spatial distribution of adsorbed atoms. We discuss in Appendix A some non-trivial aspects of the MC simulations for interacting particles.

2. Model

We assume that adsorbate atoms arrive at the surface with a given dose rate ζ. Adsorbed atoms are mobile on the surface. In the case of no interacting particles their diffusion obeys the standard equation,

$$D = D_0 \exp\left(-\frac{E_a}{k_B T}\right), \tag{1}$$

where E_a is activation energy. For the activation energy of $E_a=0.1\ eV$ typical both for Ag on MgO [9,10] and Pd [19], one gets in the typical experimental temperature interval of $T=300\div1000\ K$, that the argument of exponent, E_a/k_BT, changes only by an order of magnitude, in the interval $0.02\div0.3$. This clearly indicates that adsorbate diffusion is weakly activated which means, the observed temperature effects most probably are connected with *interactions* of adsorbed particles. As we show below, diffusion determines the scale of formed structures but not their type. In this sense, the incomplete information about diffusion coefficient pre-exponent has no big effect on the further qualitative conclusions.

Let us translate this information to the abstract level of computer simulations. We study the adsorption of particles on sites of square discrete lattice. Each site can be either empty (state 0) or occupied by an adsorbate (state A). The adsorbate concentration C_A is the fraction of occupied sites on the lattice. Our present $\boldsymbol{D}$=2 model is restricted to the growth of adsorbate monolayer, since we are interested in initial stages of thin film growth.

Processes on the lattice are stochastic, and thus could be described in terms of the Master Equation [20]. To define it, one has to specify the elementary processes. Adsorption (hereafter we follow the terminology [20]) is a *monomolecular* process, 0→A, i.e., a single site changes its state from 0 to A. The rate of this process is $\zeta=ka^2$, where k is adsorption rate per surface unit and time unit. The desorption processes A→0 are neglected in our model since experiments show that at moderate temperatures adsorption is irreversible.

Diffusion of an adsorbed particle on the lattice is described by its hops to a free nearest neighbouring (NN) site. The standard diffusion expression is

$$D = \frac{a^2}{z} d, \tag{2}$$

where $\zeta=4$ is the number of NNs and d is the so-called hopping rate. According to the terminology [20], diffusion is a typical example of the *bimolecular* process when the state of two NN sites is changed simultaneously, A0→0A, with the rate d. Both rates ζ and d have dimension of s^{-1}.

Now let us introduce an interaction between adsorbate atoms (we call them hereafter *particles*). We restrict our model by taking into account short-range interaction only between particles in NN sites. This is described by the parameter $E_{AA}=-\varepsilon$, with $\varepsilon>0$ (attraction). An interaction energy is always introduced in equations in a combination with the temperature, through the additional dimensionless parameter $\omega=\varepsilon/k_BT$. In our approach, aggregates of particles are *dynamical* formations; single particles can join and leave aggregates. This is in contrast to the standard nucleation and growth phenomenological theory [3] based on the irreversible growth of aggregates exceeding some critical size. When adsorbate atoms interact each with other, the hopping rate between two NN sites depends on the total energies of adsorbate atom in these two sites. These energies depend on pair interaction energy ε and configuration of other adsorbate atoms surrounding these two sites. This results in *energy dependence* (lateral interaction) of the kinetics under study.

To construct the Master Equation with the energy dependence, which is well known to be non-unique procedure, we use *the standard model* approach described in references [20-22]. In Appendix A we present a short description of this model. Its advantage is usage of a new axiomatic approximation to the kinetics of diffusion-controlled reversible processes. According to this approach, only reversible processes have the energetic dependence. Such a process in our model is particle diffusion (forward and backward hops). Since we neglect desorption of particles, their adsorption is an irreversible step. Accordingly, its rate is independent on the energetic, i.e. the states of the NN sites of the adsorbed particle. For any configuration of neighbouring sites the adsorption rate is chosen to be ζ.

Nontrivial problem in our model is the *pattern* formed by adsorbed particles on the lattice. The structure for a given C_A is determined by the two dimensionless parameters: ω and d/ζ. The latter is

typically quite large: $d/\zeta>>1$. Before making any MC modelling, we can expect two different types of adsorbate patterns, depending on the value of the ω parameter.

3. The scenario of the thin film growth

One can start with a system in the quasi-equilibrium state where new particles are added "adiabatically". In other words, it is assumed that due to a high mobility of adsorbed particles the metallic structure on the substrate quickly relaxes after rare events of new particle adsorptions, and thus the Gibs statistics for equilibrium structures is valid [9]. However, this in fact means that particles are only weakly interacting (small parameter ω). In this case the structure of adsorbed particles is quite trivial: particles form loose clusters where new particles join and leave these clusters easily due to their diffusion. Two spatial scales determine the adsorbate structure. The first scale is the mean distance between particles, which is determined by particle concentration C_A. The second scale is the *correlation length*, which is governed by the energetic interaction between particles. (Despite the fact that our interaction is short-range, limited by the NN particles only, nevertheless one should remember possible ordering processes due to the cooperative behaviour in many-particle system, see also [19]).

In the opposite limiting case of the large parameter ω particles are strongly bound to clusters due to their mutual attraction. Diffusion is possible only for single, just adsorbed particles. In this case system relaxation to equilibrium is hardly possible on the time scale of experiments (minutes). That is, the pattern formation is entirely determined by the *kinetics*, not thermodynamics. Namely in this regime one can expect the formation of nontrivial adsorbate structures.

We consider the last limiting case using the two methods. Firstly, we do it qualitatively, and then in the next Section 4 discuss in detail, using our MC computer simulations. We start our analysis by assuming that the parameter ω is large (which is supported by results of the MC simulations.) Some analytical estimates could be made assuming that $\omega>\omega_0$, where ω_0 is identified with the critical value ω_0 in the lattice gas model [24]. The well-known On sager solution for the $\boldsymbol{D}=2$ gas model gives $T_c=0.567\varepsilon/k_B$, i.e. the dimensionless critical $\omega_0=e/k_BT_c\approx1.764$, is of the order of unity.

For large attraction energies any encounter of a mobile particle with another one or the aggregate results in the loss of particle mobility. We assume that the particles *inside* the aggregate can relax, making it more compact and dense, but cannot leave the aggregate. Nucleation of the aggregate occurs due to the random encounter of two mobile particles. The immobile (at low temperature) dimer grows further due to permanent adsorption of new particles. Smallness of the adsorption coefficient ζ with respect to the hopping rate d makes a new encounter of the two particles quite a rare event (two newly adsorbed particles have to find each other) as compared to much more probable attachment of newly adsorbed particle to the pre-existing aggregate.

The characteristic properties of such the aggregate structure could be qualitatively described in the following simple way. Let us introduce a new parameter l_0, which is the characteristic length scale of the aggregate structure – the mean distance between nearest aggregates. We choose the time increment t_0 in such a way that only one particle is adsorbed during this period on the surface area of a size l_0: $kl_0^2t_0=1$. (That is, one can neglect an encounter of single particles.) During this characteristic time t_0 a newly created particle has to find an aggregate. This is possible if the diffusion length is close to the linear size of an area: $l_0=(Dt_0)^{1/2}$. Eliminating the parameter t_0, one finds $l_0^4=D/k$. That is, the characteristic length could be expressed in the units of lattice constant

$$L_0 = \frac{l_0}{a} = \frac{1}{a}\left(\frac{D}{k}\right)^{1/4}, \qquad (3)$$

or using Eq. (2)

$$L_0 = \left(\frac{d}{z\zeta}\right)^{1/4}. \qquad (4)$$

Surely, this is not a kind of the regular structures. The scale l_0 gives only the mean distance between aggregates. For illustration, let us consider a random distribution of such $\boldsymbol{D}=2$ aggregates with the density $n_0=1/l_0^2$ (the Poisson distribution and density fluctuations take place). If the mean radius of an aggregate,

assumed for simplicity to be of a cyclic shape, is R, one can find a simple relation between the parameter R and the adsorbant concentration C_A:

$$C_A = \pi \frac{R^2}{l_0}. \quad (5)$$

From here it follows that $R\alpha(C_A)^{1/2}$. Equation (5) is valid for small concentrations of adsorbants when one can neglect the aggregate overlapping.

It should be noted that our critical exponent of 1/4 in Eq. (4) based on the scaling arguments, differs from the exponent of 1/6 in generally accepted nucleation and growth theory [3,4]. The latter is typical mean-field rate-equation approach neglecting any effects of reactant density fluctuations. The more so, this theory is based on a standard assumption of the constant reaction rates. For the diffusion-controlled reactions these rates are supposed to be proportional to the relevant diffusion coefficients [3,4]. This idea comes from the pioneering studies by Smoluchowski (1917) [23] and it is valid, strictly speaking, only for $\boldsymbol{D}=3$ systems. In fact, the same approach shows non-steady-state reaction rates for $\boldsymbol{D}=2$ case discussed in nucleation and growth theory.

Intensive studies of last two decades have demonstrated (see [20] and references therein) that Smoluchowski approach is quite approximate since neglects effects of reactant density fluctuations. Due to this fact the mean-field theory could be applied only for space dimensions $\boldsymbol{D}\geq 4$, at lower dimensions at long times the reaction rates are not constants, even in $\boldsymbol{D}=3$. The kinetic systems behave similarly to equilibrium systems with phase transitions - the fluctuation effects change the critical exponents. This is why the critical exponent of 1/6 in the nucleation and growth theory is not backed by any serious theory (as well as MC simulations, to our knowledge).

Additional problem of the applicability of the nucleation and growth theory is its neglect of the adsorbate atom interaction. Let us just quote a special study performed for Ag on Pt(111) surface [19]: "interaction of NN adsorbed atoms leads to metal island densities over an order of magnitude larger than those predicted by nucleation theory and identify a severe limitation of its applicability."

Note also that the exponent of 1/4 in, Eq. (4), does not result from any mean-field theory but from the scaling arguments. Its final proof could be done only by means of direct MC simulations, presented in our paper.

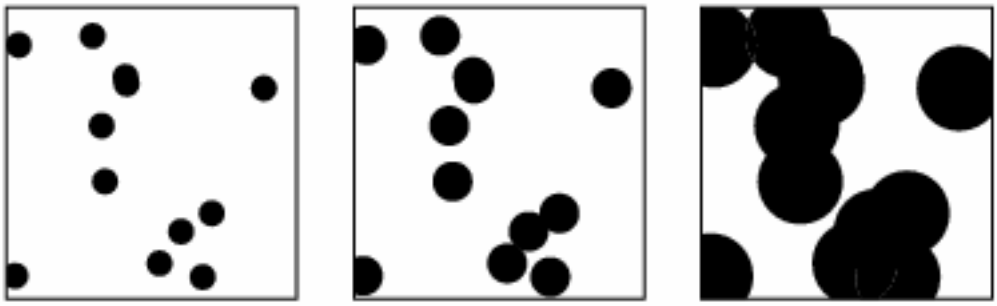

Figure 1. Schematic model of the growth of adsorbate aggregates with randomly chosen nucleation sites. Exchange of particles between aggregates is neglected.

The effect of aggregate overlapping (coalescence of small clusters into larger clusters) as small clusters grow could be easy illustrated. Figure 1 shows a random distribution of points, which serve as nucleation centres of the clusters (circles of equal radii). It is obvious that due to the Poisson fluctuations some of the nearest circles start to overlap due to influx of new particles (formation of larger aggregates). That is, large aggregates of irregular shape arise from overlap of several small aggregates. As a result, we obtain the characteristic distribution of aggregates, which is similar to results of actual MC computer simulation presented below for large ω. Note that this pattern is entirely defined by the kinetics, not thermodynamics.

4. The restrictions of MC simulations

Using the standard Ag diffusion parameters, $E_a=0.1$ *eV*, $D_0=10^{-3}cm^2s^{-1}$, and the adsorption rate $k=2\div 8\ 10^{13}\ Ag/cm^2s$ [5], from Eq. (3) one can easy estimate the mean distance between aggregates to be

several hundred of lattice constants, which coincides with the characteristic distance between cluster centres estimated from experiments, as mentioned in the Introduction (*0.1 μm*). However, direct MC simulations are hardly possible for determining the aggregate sizes L_0. Indeed, for a good statistics one has to use in simulations a lattice with the linear size $L>>L_0$, which is unrealistic in this case. One has to remember also that the computational time in MC simulations is proportional to L^2D.

Nevertheless, one can study the characteristic stages of aggregation exploiting the scaling arguments. Let us use the system of units such that $\zeta=1$. (Transition to the new units simply means that time is measured no longer in seconds but in units of $\tau=\zeta^{-1}$.) It follows from Eq. (4) that an increase of the hop frequency d (or diffusion coefficient D) by a factor of $2^4=16$ (with the scaling factor $d'=2^4d$) has to lead to the increase of the characteristic distance between aggregates by a factor of two (scaling is $L'_0=2L_0$). If simulations confirm this, then in real case one expects to find similar aggregate structures but larger in size.

Let us estimate available computer facilities. We choose the lattice size of $L=2^8=256$ sites and a maximal value of hop frequency $d'=2^9\,10^3$ (respectively, $d=2^5\,10^3$). One MC simulation run with d' takes approximately 24 hours on Alpha 21164 workstation. Using Eq. (4), one can estimate that the parameter d corresponds to the characteristic distance between aggregates of the order of $L_0\approx10$. That is, the aggregate scale L_0 fulfils the condition $L>>L_0$, which ensures a good statistics in MC simulations. At the same time, the length L_0 is large enough to observe the aggregate formation.

5. Simulation algorithm

Our model includes adsorbtion, diffusion and interaction of particles. As was shown [22], it is very convenient to use in the MC simulations the so-called *pair algorithm*. The basic idea of the algorithm is to consider *two* NN sites and account for all possible processes therein. This determines the maximal time update.

In the MC simulations we use the following steps:

1) The maximal time update is determined from the processes:

   A0: jump of A + adsorption in 0 $\quad p_1=2d+\zeta,$ (6)

   00: adsorption in 0 + adsorption in 0 $\quad p_2=2\zeta,$ (7)

   AA: configuration does not change $\quad p_3=0,$ (8)

   as a $\Delta t=1/\max(p_i)$. In the considered model, when $d>>\zeta$, the time update is determined by the diffusion (hopping rate d) and thus $\Delta t=1/p_1$.
2) The simulation time is updated, $t\rightarrow t+2\Delta t/L^2$.
3) Horizontal or vertical orientation of a pair on a lattice is chosen randomly.
4) The pair is placed randomly in the lattice.
5) The state of the pair is analysed. According to the configuration of the pair, one of independent processes in Eqs. (6-8) is started randomly with the appropriate weight.
   a) Hopping step. Firstly, an energy difference is calculated between the final and initial reactant states, $\Delta\omega=\omega_\beta-\omega_\alpha$. Secondly, a RN is generated and if $RN<1/[1+\exp(\Delta\omega)]$ the hop step is completed, otherwise the configuration stays unchanged.
   b) Adsorption step. A particle is adsorbed in the corresponding empty site.
6) The program returns to step 2) if time t is less than the final simulation time.

6. Results

Let us consider firstly the results for the large value of the dimensionless attraction energy $\omega=3$ (strong attraction and/or low temperatures). Four windows in Fig. 2 correspond to monotonous increase of adsorbate concentration. It is obvious that the qualitative picture discussed above indeed takes place. The adsorbate aggregates are very dense with only a few small holes. These aggregates are practically immobile, and no new aggregates arise. That is, all newly adsorbed particles join already existing aggregates. Small aggregates grow independently and coalesce periodically when their boundaries touch, thus forming large aggregates of irregular shape. An increase of the diffusion coefficients by a factor of $2^4=16$ increases twice the characteristic distance between aggregates (Fig. 3) but preserves the pattern similarity. These aggregate structures are quantitatively analysed below using the joint correlation functions.

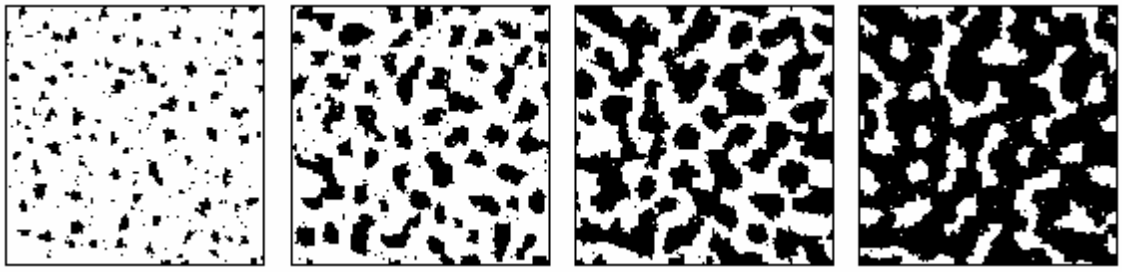

Figure 2. Spatial distribution of adsorbate concentrations: $C_A=0.1$ (a), *0.3* (b), *0.5* (c), *0.7* (d). $\omega=\varepsilon/k_BT=3$.

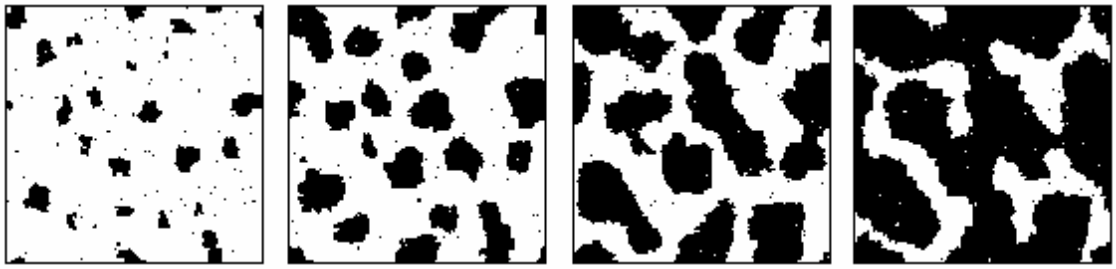

Figure 3. The same as Fig. 2 with the hopping rate increased by a factor of 2^4=16.

The aggregate pattern remains similar after decrease of the interaction energy down to $\omega=2$, $d=2^9$ 10^3. However, aggregates become here looser (Fig 4). One can observe also a large number of single particles, which leave aggregates and walk on the lattice. Further decrease of the dimensionless attraction energy down to the critical value of $\omega=1.25$ leads to the disappearance of aggregate pattern Fig 5: one can see only the short-range order in the distribution of particles (many very small and loose aggregates).

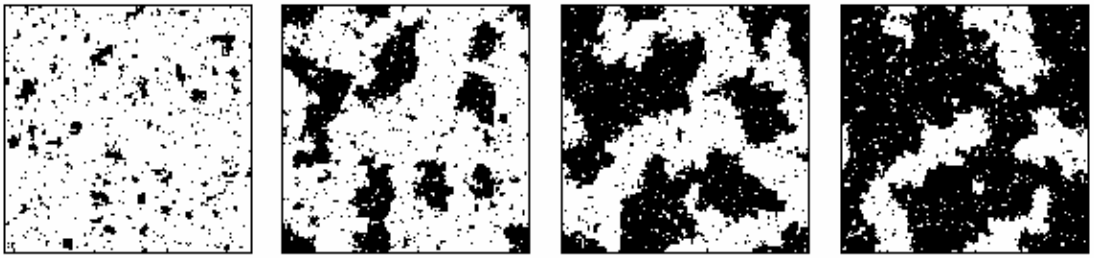

Figure 4. The same as Fig 2 for $\omega=2$.

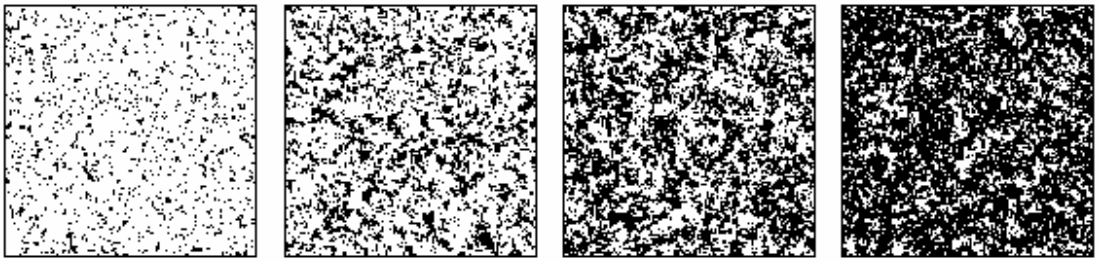

Figure 5. The same as Fig 2 for $\omega=1.25$.

Now let us characterize the aggregate patterns quantitatively, using the language of the *joint correlation functions* $F_{\alpha\beta}(r)$ where α, β=0, A [20]. These functions have a simple physical meaning. Assume that some site is in the state α=0, A. We are interested to find a probability that a site at the distance r is in the state β. This probability, $\omega_\beta^{(\alpha)}(r)=F_{\alpha\beta}(r)\ C_\beta(r)$, is normalized to unity,

$$\sum_{\beta=0,A} \omega_{\beta}^{(\alpha)}(r) = 1 . \tag{9}$$

Two equations follow from Eq. (9),

$$\begin{aligned} F_{0A}(r)C_A + F_{00}(r)C_0 &= 1, \\ F_{AA}(r)C_A + F_{A0}(r)C_0 &= 1 . \end{aligned} \tag{10}$$

Taking into account the symmetry properties $F_{0A}(r) = F_{A0}(r)$, the conclusion could be drawn that of all these functions only one is independent. Therefore, for the illustration hereafter we consider only the function $F_{AA}(r)$, which describes the correlations in distribution of adsorbate atoms.

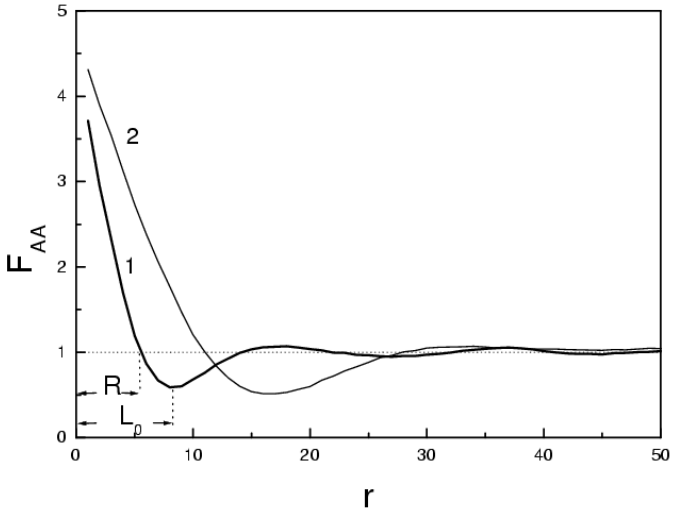

Figure 6. The joint correlation function vs the relative distance between adsorbate atoms (in units of lattice constant): $\omega=3.0$, $C_A=0.1$, hop frequency $d=2^5\ 10^3$ (curve 1) and $d'=2^9\ 10^3$ (curve 2).

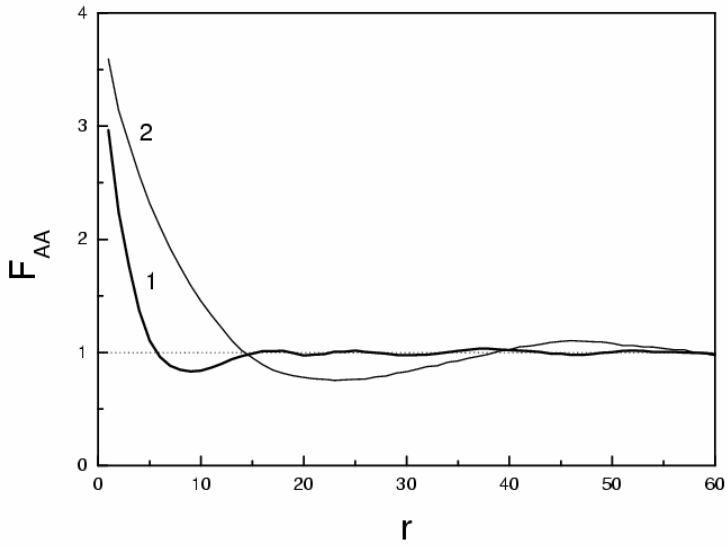

Figure 7. The same as Fig. 6 for $\omega=2.0$.

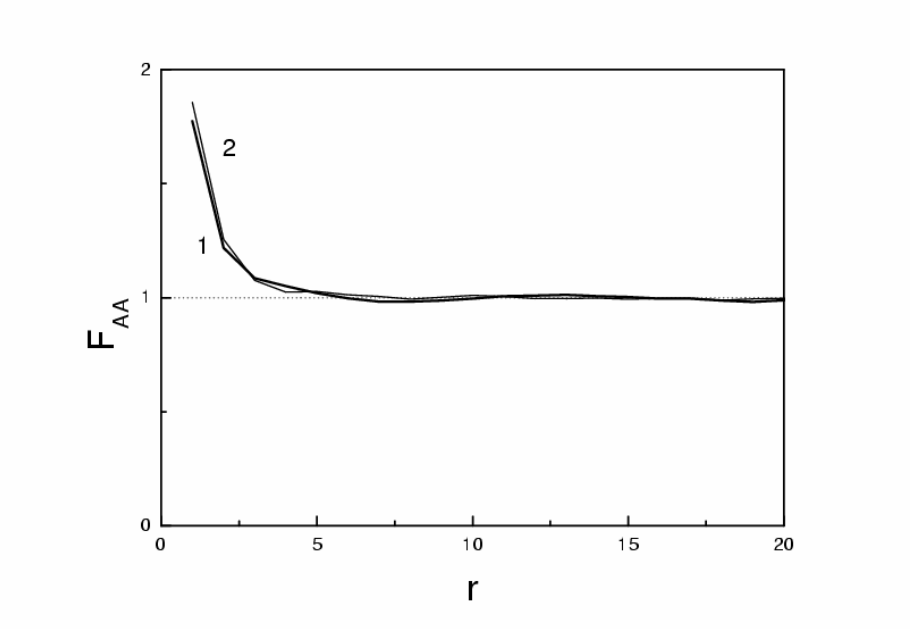

Figure 8. The same as Fig. 6 for $\omega=1.25$.

Figures 6 to 8 demonstrate the correlation functions for three above-discussed situations for decrease of the dimensionless particle interactions $\omega=3, 2$, and lastly down to 1.25. In particular, Fig. 6 shows clearly how the aggregate distribution is described in terms of the correlation function. Let us take some particle A. With high probability it belongs to some aggregate and is surrounded by other particles A. The correlation function gives the probability density to find a particle A at a given distance r from the chosen particle placed into the origin. The random (chaotic, or Poisson) distribution corresponds to $F_{AA}(r)=1$.

A figure 6 shows that at small relative distances the correlation function greatly exceeds the unity thus indicating a strong aggregation. From here one can define the aggregate radius R as the distance where the correlation function approaches to the unity. At larger distances the correlation function becomes even less than unity: there are no other particles nearby the aggregate boundary since all such particles are already attached. Lastly, with further increase of the distance, the correlation function reaches the asymptotic value of the unity once more, which indicates the presence of other aggregates at larger distances. The distance r where it takes place corresponds to the mean distance between aggregates, L_0, introduced above. Let us define L_0 from the minimum of the correlation function. One can see that for the hopping rate of $d=2^5\ 10^3$ (curve 1) the aggregate radius R is about 5 lattice constants, and the scale L_0 is about 8. After the scaling (curve 2) the shape of the correlation function remains the same, but both scales, R, L_0, increase twice. This is in the complete agreement with above-made scaling arguments.

For $\omega=2.0$ (Fig. 7) we obtain qualitatively similar correlation functions with less pronounced minima due to reduced aggregate density. The scale L_0 is still observable and it has the same order of magnitude. However, for smaller $\omega=1.25$ (Fig. 8) the aggregate structure completely disappear, L_0 is no longer observable, and the scale R (the mean size of the aggregate) loses the dependence on the hop frequency (which indicates the quasi-equilibrium regime).

7. Discussion and conclusions

Our MC modelling demonstrates a considerable difference between simulations assuming the adsorbate concentration to be constant, and for a permanent flux of adsorbates to the surface. The principle point is that adsorbate-adsorbate interactions at relatively low temperatures keep most of particles in their aggregates, which are highly non-equilibrium. This is why no Ostwald-type ripening of small aggregates into larger aggregates takes place at the experimentally observable time scale. In our submonolayer adsorbate modelling, we observe loose adsorbate aggregates for the dimensionless attraction energy $\omega=E_a/k_BT>1.25$, and no pattern formation at smaller interaction energies/higher temperatures. Our modelling neglects a role of point defects/impurities, which often assumed to serve as

nucleation sites for aggregates. This is true under following conditions. Let the mean distance between defects is L_d, which is defined by their concentration. If $L_d > L_0$, defects play no role; just adsorbed particles with greater probability meet and join pre-existing aggregates. For high defect concentrations, $L_0 > L_d$, just adsorbed particles meet defects, and form immobile dimers. For aggregation of other particles such dimers serve very similarly to the result of the encounter of the two mobile adsorbate atoms. As a result, one can expect growth of many small adsorbate aggregates rather than large aggregates. According to our estimates for L_0 presented above and experiments, critical surface defect concentration for Ag/MgO could be of the order of 10^{-4} (in dimensionless units).

To learn more about adsorbate growth mode, one has to go beyond $\boldsymbol{D}=2$ simulations and model a growth of several metal planes, which is now in progress.

Acknowledgements

Fonds der Chemischen Industrie and the European Center of Excellence in Advanced Materials Research and Technology supported part of this work. (Contract No ICA-1-CT-2000-7007)

Appendix A

A.1. DETAILED BALANCE PRINCIPLE

The kinetic processes, such as particle (atom, molecule or defect) adsorption, desorption and diffusion, are treated traditionally in terms of the Master Equation (ME). This serves as a general axiomatic approach and basis for both analytical kinetic methods (MF, Cluster approximation, etc. [20]) and MC computer simulations. ME is formally defined if all possible system`s states and relevant transition rates are known. It is sufficient to know the transition rates $K(\alpha \rightarrow \beta)$ for elementary transitions from the (conditional) initial state α to the final state β.

The elementary processes include along with the above-mentioned adsorption, desorption and diffusion, also *reactions* between particles. When generalizing kinetic theory through the incorporation of particle lateral (energetic) interaction, the dependence of the transition rates on the particle interaction and diffusion energies and temperature should be specified, which is not unique procedure. Let us consider for the illustration a couple of elementary processes: system's forward and backward transitions, $\alpha \leftrightarrow \beta$. The kinetics of this extremely simplified process reads

$$\frac{dW(\beta)}{dt} = -\frac{dW(\alpha)}{dt} = K(\alpha \rightarrow \beta)W(\alpha) - K(\beta \rightarrow \alpha)W(\beta). \qquad \text{(A.1)}$$

Here $W(\alpha)$ and $W(\beta)$ are probabilities to find the system in the states α and β, respectively; $W(\alpha)+W(\beta)=1$. The local equilibrium, $W^{eq}(\alpha)$ and $W^{eq}(\beta)$, is reached asymptotically, as $t \rightarrow \infty$. Even in this simplest case the transition rates are not uniquely defined. The point is that the steady-state solution of Eq. (A.1) is defined not by the individual transition rates, but by their *ratio* only:

$$\frac{K(\alpha \rightarrow \beta)}{K(\beta \rightarrow \alpha)} = \frac{W^{eq}(\beta)}{W^{eq}(\alpha)}. \qquad \text{(A.2)}$$

The detailed balance principle (DBP), Eq. (A.2), imposes only a weak restriction on the transition rates [25]. Their unique definition needs use of an *additional* relation between the rates. Besides, DBP holds only for *reversible* processes. That is, if in a couple of related processes one of them, e.g., desorption, could be neglected, the transition rate for another process (adsorption) is in fact undefined.

Obviously, DBP is unable to introduce particle lateral interaction into the ME formalism. This uncertainty clearly indicates that the DBP-based theory is incomplete. Completion of the axiomatic theory is not a kind of problem, which could be solved using purely physical arguments. A similar situation occurs in theory of stochastic differential equations [26] where the same equations are interpreted (i.e. defined) following either Ito or Stratonovich. The *interpretation* in fact means the choice of additional definitions, that is, use of different axiomatic. Such use of different axiomatic, necessary for unique definition of the transition rates in the ME formalism, leads to a simultaneous co-existence of a number of so-called *dynamics* (Metropolis, Glauber, etc. [27]). Unlike quantum mechanics, where change of dynamics from Schrödinger to Heisenberg does changes the basic mathematical formalism, but not

physical results, the change of dynamics in the ME affects the results. If the irreversible processes are involved, the results of different dynamics may differ qualitatively. The variety of dynamics and their simultaneous use demonstrate clearly the weakness of the ME axiomatic for interacting particles rather the strength of the logics.

A.2. UNIVERSAL AXIOMATIC APPROACH

Taking into account the growing interest of scientific community to a role of particle interactions in the reaction kinetics, a number of researchers facing the mentioned ME incompleteness and giving each time their subjective solution to the problem continuously increases. As a result, even now a comparison of the results obtained by different groups is hardly possible. We do believe that a real solution is a transition to a *universal* theory. Let us formulate the basic principles of such universal axiomatic approach. (a) Weak DBP condition has to be replaced by a stronger one, thus removing the above-described theory incompleteness. (b) This new condition has not only automatically to satisfy the DBP but is also more informative.

Since this condition is axiomatic, it cannot be derived by any physical arguments. However, it has to meet the following general axiomatic principles [25]: (i) this new definition is universal, i.e. independent on the particular physical nature of the α and β states. (ii) Taking into account that the definition of the α and β states is relative, the additional definition has to be *symmetric* with respect to exchange of α and β states. (iii) The additional definition has not only to define uniquely the transition rates for the reversible process but also the transition rate dependence on the lateral particle interaction for the irreversible processes. These latter could be treated as a limiting case of reversible processes when one of the reaction rates (forward or backward) strives for zero.

Analysis of the literature demonstrates very well how these quite general principles are systematically violated, starting with the pioneering MC study of the surface-controlled kinetics [13,28], and finishing with very typical papers [29,30] which we will discuss in more detail.

In these papers a general definition (i) is replaced by a set of particular relations for each elementary process. For instance, diffusion could be treated in terms of Metropolis dynamics whereas adsorption/desorption are described by some other dynamics [29]. The same author in his next paper [30] treats diffusion using this time the so-called Initial-State (IS) dynamics. Other people prefer the Kawasaki dynamics [31-33] (coinciding in this particular case with Glauber dynamics [34]). This arbitrary choice of the dynamics was stressed by Zhdanov [30]: "If necessary, one can use another dynamics for diffusion... the qualitative conclusions are expected to be independent on the details of the dynamics as long as it satisfies the detailed balance principle". The last statement is quite questionable since the kinetic models have to treat not only reversible processes (where DBP holds) but also irreversible processes where the kinetics is quite far from equilibrium. Lack of physical criteria for the dynamics choice immediately leads to arbitrary combinations of various dynamics. In some cases researchers use definitions of the forward and backward transition rates based on *different* dynamics [35] even not realizing that the DBP is thus violated.

As to the above-mentioned point (ii), typically there is no symmetry in the treatment the initial and final states. Quite often some authors assume that the lateral interactions determine the forward process, whereas their opponents assume that this is backward process. For example, the energetic interaction was assumed to define only desorption in reference [29], but the opposite was assumed in reference [35]. To justify this asymmetry, the so-called *transition state theory* is often mentioned [24]. This theory operates with a purely intuitive assumption on the so-called *activated states* (not used in the original definition of considered models). These latter are characterized by the undefined parameter $\omega=0\div1$ (known also as the Brønsted-Polanyi coefficient [36]). This uncertainty is a direct consequence of the logically incomplete theory [25]. Its additional definition is substituted by a speculative choice of a particular parameter ω. In this way one develops the alternative dynamics, which differ by the ω value. The ω variation allows one to transfer the energy dependence from the transition rate of the forward process to that of backward process, and vice versa. However, fans of this theory do not realize that in fact this is based on the same DBP, Eq. (A.2). This is why this theory is also logically incomplete, as well as the ME transition rates.

As to the point (iii), the situation is also uncertain. Since the DBP does not hold for irreversible processes, the energetic dependence of the transition rate becomes completely undefined. Say, the particular choice of this dependence was combined in references [13,28] with use of the phenomenological parameter $\gamma=0\div1$ (switch off/on). A similar definition was used also in reference [37] for another irreversible, decomposition process. Zhdanov [29] has stressed the arbitrary choice of the

energetic dependence by saying: "The effect of lateral interactions on the decomposition is for simplicity neglected (if necessary, it can be taken into account...)". More than once repeated "if necessary" indicates a strong need in the universal generally accepted axiomatic theory.

A.3. STANDARD DYNAMICS

We do believe that our *standard model* (*standard dynamics*) [20-22] could serve as such universal theory satisfying all three above-mentioned conditions, (i) to (iii). For *all* the elementary processes the only additional strong definition was introduced

$$\begin{aligned} K(\alpha \to \beta) &= QW^{eq}(\beta), \\ K(\beta \to \alpha) &= QW^{eq}(\alpha), \end{aligned} \tag{A.3}$$

where Q is a co-factor independent of α, β state energies. In other words, Eq. (A.3) imposes the restriction on the transition rates since Q is different for different coupled processes. As we show below, Eq. (A.3) leads to the *unique* definition of the ME, independently of the inclusion or neglect of the lateral energetic interaction.

A.4. EXAMPLES FOR THE STANDARD MODEL

Since we deal with the kinetic models based on particle diffusion and adsorption often neglecting desorption, let us illustrate use of the standard dynamics for these processes. Let us first consider elementary processes of the system transition from the state α to β. We consider (a) particle diffusion as hops between lattice sites, (b) atom adsorption/desorption on the arbitrary lattice site. In the case (a) the system is closed, i.e. the number of particles is constant (one). During the particle diffusion its environment varies, thus changing the interaction energy between particle and its surrounding, E_α to E_β. In the case (b) the system is open, the state α mean absence of particles on the surface (empty sites), whereas the state β means the adsorbed particle interacting with its environment. Since in both cases we consider the only particle, which could be in the two possible states, the local equilibrium probabilities are quasi-fermionic:

$$\begin{aligned} W^{eq}(\beta) &= f(\varphi, \mu), \\ W^{eq}(\alpha) &= 1 - f(\varphi, \mu), \end{aligned} \tag{A.4}$$

where in the case (a) $\mu=0$, but it is non-zero in the case (b). Here the function

$$f(\varphi, \mu) = \frac{1}{\exp\left((\varphi - \mu)/k_B T\right) + 1} \tag{A.5}$$

contains the chemical potential μ and the energy parameter $\varphi=E_\beta-E_\alpha$. Note that in a general case (e.g., dimer (molecule) adsorption) these probabilities have a different functional form [20,21].

To define the co-factor Q, let us consider the limiting case of pure surface when there exist no other particles around the mobile particle. This corresponds formally to $\varphi=0$ in Eq. (A.5). Denoting the diffusion rate on pure surface as d, and keeping in mind the conservation of particle number ($\mu=0$), and $f(0,0)=1/2$, one gets from Eq. (A.3)

$$\lim_{\varphi \to 0} K(\alpha \to \beta) = d = Qf(0,0) = \frac{Q}{2}. \tag{A.6}$$

As a result, we obtain for the diffusion rate

$$K(\alpha \to \beta) = 2df(\varphi, 0) = \frac{2d}{\exp\left(\varphi / k_B T\right) + 1}. \tag{A.7}$$

This coincides with the GL dynamics [34] and also agrees with the dynamics choice in references [13,28]. According to the interpretation of the case (b), the limit of $\varphi=0$ for the transition rate $K(\alpha \to \beta)$ gives the adsorption rate p on the pure surface

$$\lim_{\varphi \to 0} K(\alpha \to \beta) = p = Qf(0,\mu). \tag{A.8}$$

For the backward process of particle desorption from the pure surface with the rate k

$$\lim_{\varphi \to 0} K(\beta \to \alpha) = k = Q[1 - f(0,\mu)]. \tag{A.9}$$

This leads to a set of two equations with two variables, Q and μ, from where we obtain

$$\mathrm{Q} = \mathrm{p} + \mathrm{k}, \tag{A.10}$$

$$\frac{p}{k} = \frac{f(0,\mu)}{1 - f(0,\mu)}. \tag{A.11}$$

Equation (A.11) defines the μ parameter through the ratio of adsorption/desorption rates on a pure surface:

$$\exp\left(\frac{\mu}{k_B T}\right) = \frac{p}{k}. \tag{A.12}$$

Thus, we finally obtain

$$K(\alpha \to \beta) = \frac{p + k}{\exp(\varphi / k_B T)k / p + 1}, \tag{A.13}$$

$$K(\beta \to \alpha) = \frac{p + k}{\exp(-\varphi / k_B T)p / k + 1}. \tag{A.14}$$

Such transition rates are not known in the literature on process dynamics. One can easily check that definition, Eq. (A.2), always gives the transition rate limited from above by Q. This solves a long-standing dynamics problem. Note that trying to avoid this problem, non-analytical (in energy) expressions were used in the MP dynamics [27].

Equations (A.13) and (A.14) allow to establish an important detail of the standard dynamics, how to define the energy dependence of the transition rate for the irreversible processes. In our case neglect of desorption corresponds to $k \to 0$. From our two basic equations one obtains

$$\lim_{k \to 0} K(\alpha \to \beta) = p, \tag{A.15}$$

$$\lim_{k \to 0} K(\beta \to \alpha) = 0, \tag{A.16}$$

irrespectively the parameter φ (i.e. for arbitrary particle environment). In other words, one can neglect the energy dependence of the transition rate for irreversible process.

Note in conclusion that in our standard dynamics both forward and backward rates have the energetic dependencies, which arises directly from the above-mentioned symmetry of the theory. However, as follows from Eq. (A.16) (see also [20,21]), if one of the two adsorption/desorption rates on the pure surface is much lower than another rate, the energy dependence is pronounced mainly for the low-rate process. In this sense the energy dependence derived using the standard dynamics, turns out to be really dynamical.

References

[1] Henrich V.E., Cox P.A. (1994) *The Surface Science of Metal Oxides*. Cambridge: Cambridge Univ. Press, England.

[2] Ertl G., Freund H.-J. (1999) *Physics Today* **1**, 32.

[3] Venables J.A. (2000) *Introduction to Surface and Thin Film Processes*. Cambridge: Cambridge Univ. Press, England

[4] Brune H. (1998) *Surf. Sci. Reports* **31**, 121.

[5] Larsen J.H., Ranney J.T., Starr D.E., Musgrove J.E., Campbell C.T. (2001) *Phys. Rev.* B **63,** 195410.
[6] Haas G., Menck A., Brune H., Barth J.V., Venables J.A., Kern K. (2000) *Phys. Rev.* B **61**, 11105.
[7] Harada T., Asano M., Mizutani Y. (1992) *J. Cryst. Growth* **116,** 245.
[8] Trampert A., Ernst F., Flynn C.P., Fishman H.F., Rühle M. (1992) *Acta Metall. Mater.* **40**, S227.
[9] Fuks D., Dorfman S., Kotomin E.A., Zhukovskii Yu.F., Stoneham A.M. (2000) *Phys. Rev. Lett.* **85**, 4333.
[10] Fuks D., Kotomin E.A., Dorfman S., Zhukovskii Yu.F., Stoneham A.M. (2002) *Surface Science* **499**, 24.
[11] Zhdanov V.P., Kasemo B. (1999) *Surf. Sci.* **437**, 307.
[12] Zhdanov V.P. (2001) *Eur. Phys. J.* B **19**, 97.
[13] Silverberg M., Ben-Shaul A. (1987) *J. Chem. Phys.* **87,** 3178.
[14] Becker O.M., Silverberg M., Ben-Shaul A. (1990) *Israel J. Chem.* **30**, 179.
[15] Zangwill A., Kaxiras E. (1995) *Surface Science Letters* **326**, L483.
[16] Bartelt M.C., Stoldt C.R., Jenks C.J., Thiel P.A., Evans J.W. (1999) *Phys. Rev.* B **59**, 3125.
[17] Amar J.G., Family F., Lam P.-M. (1994) *Phys. Rev.* B **50**, 8781.
[18] Ratsch C., Zangwill A., Šmilauer P., Vvedensky D.D. (1994) *Phys. Rev. Lett.* **72**, 3194.
[19] Fichthorn K.A., Scheffler M. (2000) *Phys. Rev. Lett.* **84**, 5371.
[20] Kotomin E.A., Kuzovkov V.N. (1996) *Modern Aspects of Diffusion-Controlled Reactions: Cooperative Phenomena in Bimolecular Processes* vol. **34**, Comprehensive Chemical Kinetics. Amsterdam: North Holland, Elsevier.
[21] Mai J., Kuzovkov V.N., Niessen W.von (1996) *J. Phys. A: Math.Gen.* **29**, 6205.
[22] Zvejnieks G., Kuzovkov V.N. (2001) *Phys. Rev.* E **63,** 051104.
[23] Smoluchowski M. (1917) *Zs. Phys. Chem. Abt.* B **92**, 129.
[24] Zhdanov V. (1991) *Elementary Physicochemical Processes on Solid Surfaces*. Plenum NewYork.
[25] Kuzovkov V., Zvejnieks G. (2002) *Phys. Rev.* E **65**, 033102.
[26] Gardiner C. (1983) *Handbook of Stochastic Methods for Physics, Chemistry and the Natural Sciences*. Berlin: Springer.
[27] Binder K., Heermann D. (1988) *Monte Carlo Simulation in Statistical Physics*. Berlin: Springer.
[28] Silverberg M., Ben-Shaul A. (1987) *Surf. Sci.* **214**, 17.
[29] Zhdanov V. (1999) *Phys. Rev.* E **59**, 6292.
[30] Zhdanov V. (2001) *Phys. Rev.* E **63**, 011908.
[31] Kawasaki K. (1966) *Phys. Rev.* **145**, 224.
[32] Kawasaki K. (1966) *Phys. Rev.* **148**, 375.
[33] Kawasaki K. (1966) *Phys. Rev.* **150**, 385.
[34] Glauber R. (1963) *J. Math. Phys.* **4**, 294.
[35] Kaukonen H.-P., Nieminen R. (1989) *J.Chem. Phys.* **91**, 4380.
[36] Nørskov J.K. Stoltze P. (1997) *Handbook of Heterogeneous Catalysis* vol **3**, ed G. Ertl *et al.* Weinheim: Wiley.
[37] Zhdanov V., Kasemo B. (1996) *J. Chem. Phys.* **104**, 2446.

Received on the 4th of February 2004

Computer Modelling & New Technologies, 2004, Volume 8, No.1, 20-23
Transport and Telecommunication Institute, Lomonosov Str.1, Riga, LV-1019, Latvia

NONLINEAR PROBLEM OF A THERMAL CONDUCTIVITY IN A SOLID CYLINDER

I. B. FRENKEL

Industrial Engineering and Management Department,
Negev Academic College of Engineering,
Beer Sheva 84100, Israel, E-mail: iliaf@nace.ac.il

Method of perturbations [2], [4] can be applied with great success to the solution of the boundary-value problems of thermal conductivity, solved by an integration of the nonlinear differential equations. In the paper we propose the combination of the small parameter method and method of perturbations for solution of a nonlinear problem of a thermal conductivity in the cylinder under condition of a linear dependence of thermal conductivity factors and a thermal capacitance on temperature.
Keywords: thermal conductivity, heat conduction equation, mathematical methods

Let us consider a nonlinear thermal conductivity problem in a solid cylinder with height L and radius R with interior radiant. The dependence of a thermal conductivity factor and a thermal capacitance on temperature is under the following law:

$$c(T) = c_0(1+\varepsilon_1 T)\,, \tag{1}$$

$$\lambda(T) = \lambda_0(1+\varepsilon_2 T)\,, \tag{2}$$

where $c_0, \lambda_0, \varepsilon_1, \varepsilon_2$ - constants.

Let us consider the heat conduction equation in the following way:

$$c(T)\frac{\partial T}{\partial \tau} = \mathrm{div}[\lambda(T)\nabla T] + f_0\,, \tag{3}$$

while boundary conditions are as following:

$$T\big|_{\tau=0} = T_0 = const\,, \tag{4}$$

$$\alpha\left(T - T_H\right) + \lambda(T)\left.\frac{\partial T}{\partial r}\right|_{r=R} = 0\,, \tag{5}$$

$$\left.\frac{\partial T}{\partial z}\right|_{z=0} = 0\,, \tag{6}$$

$$\alpha\left(T - T_H\right) + \lambda(T)\left.\frac{\partial T}{\partial z}\right|_{z=L} = 0\,. \tag{7}$$

Here α is a heat-transfer coefficient, which takes into account thermal stream from a wall of the cylinder to an environment with temperature T_H.

Let's accept ε_1 for small parameter and we shall enter a new variable t under the law $t = T - T_H$. After simple transformation the equations (3)-(7) will become:

$$\frac{1}{\alpha_0}\frac{\partial t}{\partial \tau} = \Delta t + \varepsilon_1 F(t) + F_0, \tag{8}$$

where $F_0 = \frac{f}{\lambda_0}$, $\alpha_0 = \frac{\lambda_0}{c_0}$ and $F(t) = -(F_0 + \frac{\partial t}{\partial \tau})(t + T_H) - T_H(1 - \frac{\varepsilon_2}{\varepsilon_1})\Delta t + \frac{\varepsilon_2}{\varepsilon_1}(\Delta t)^2$,

$$t\big|_{\tau=0} = T_0 - T_H = t_0 = const, \tag{9}$$

$$\alpha t + \lambda(t)\frac{\partial t}{\partial r}\bigg|_{r=R} = 0, \tag{10}$$

$$\frac{\partial t}{\partial z}\bigg|_{z=0} = 0, \tag{11}$$

$$\alpha t + \lambda(t)\frac{\partial t}{\partial z}\bigg|_{z=L} = 0. \tag{12}$$

The solution of equations (8) - (12) will be in the form of:

$$t = t_1 + \varepsilon_1 t_2. \tag{13}$$

Then (8) - (12) will become two systems for two approximations:

For the first approximation

$$\begin{cases} \dfrac{1}{\alpha_0}\dfrac{\partial t_1}{\partial \tau} = \Delta t_1 + F_0 \\ t_1\big|_{\tau=0} = t_0 \\ \alpha t_1 + \lambda_0 \dfrac{\partial t_1}{\partial r}\bigg|_{r=R} = 0 \\ \dfrac{\partial t_1}{\partial z}\bigg|_{z=0} = 0 \\ \alpha t_1 + \lambda_0 \dfrac{\partial t_1}{\partial z}\bigg|_{z=L} = 0 \end{cases}$$

For the second approximation

$$\begin{cases} \dfrac{1}{\alpha_0}\dfrac{\partial t_2}{\partial \tau} = \Delta t_2 + F(t_1) \\ t_2\big|_{\tau=0} = 0 \\ \alpha t_2 + \lambda_0 \dfrac{\partial t_2}{\partial r}\bigg|_{r=R} = \alpha \dfrac{\varepsilon_2}{\varepsilon_1}(t_1 + T_H)t_1\bigg|_{r=R} \\ \dfrac{\partial t_2}{\partial z}\bigg|_{z=0} = 0 \\ \alpha t_2 + \lambda_0 \dfrac{\partial t_2}{\partial z}\bigg|_{z=L} = \alpha \dfrac{\varepsilon_2}{\varepsilon_1}(t_1 + T_H)t_1\bigg|_{z=L} \end{cases} \tag{14)-(15}$$

For a solution of systems (14) - (15) we shall take advantage of a method of final integrated transformations [1]. Kernels of the transformations, as shown in [3], are identical to the equations, defining various approximations to a required solution.

For elimination of differential operations on z under the set boundary conditions we obtain a kernel of integrated transformation:

$$P_1 = \frac{1}{C_n}\cos \mu_n z, \tag{16}$$

where $C_n = \frac{L}{2} + \frac{\sin^2(\mu_n L)}{4\mu_n}$ and μ_n is the positive solutions of an equation

$$\cot(\mu_n L) = \frac{\mu_n L}{Bi_1}, \quad n = 1, 2, \ldots \tag{17}$$

$Bi_1 = \dfrac{\alpha L}{\lambda_0}$ - Biot number.

Final integrated transformation with kernel P_1 of function t_i, (i=1,2) we shall designate as $\overline{t_i}$. Then

$$\overline{t_i} = \frac{1}{C_n}\int_0^L t_i \cos(\mu_n z)dz \,. \tag{18}$$

According to (18) we shall obtain:

$$\overline{t_0} = \frac{1}{C_n}\int_0^L t_0 \cos(\mu_n z)dz = \frac{t_0}{\mu_n C_n}\sin(\mu_n L)\,. \tag{19}$$

For elimination of differential operations on r under the set boundary conditions we obtain a kernel of integrated transformation as:

$$P_2 = \frac{1}{C_m} rJ_0(\nu_m r)\,, \tag{20}$$

where $C_m = \dfrac{R^2}{2}J^2{}_1(\nu_m R)\left[1+\left(\dfrac{Bi_2}{\nu_m R}\right)^2\right]$, $J_0(\nu_m r)$ are Bessel's functions of the first kind (zero order), ν_m are solutions of an equation,

$$Bi_2 J_0(\nu_m R) - \nu_m R J_1(\nu_m R) = 0\,, \tag{21}$$

$J_1(\nu_m R)$ - Bessel's functions of the first kind (first order), $Bi_2 = \dfrac{\alpha R}{\lambda_0}$ - Biot number.

Final integrated transformation with kernel P_2 of the function t_i, (i=1,2), we shall designate as t_i^*. Then

$$t^*{}_i = \frac{1}{C_m}\int_0^R \overline{t_i} rJ_0(\nu_m z)dz\,, \tag{21}$$

Applying sequentially to systems (14) and (15) transformations with kernels (16) and (20), we shall obtain:

$$\frac{1}{\alpha_0}\frac{\partial t_1^*}{\partial r} + (\mu_n^2 + \nu_m^2)t_1^* = F_0^*\,, \tag{22}$$

$$\frac{1}{\alpha_0}\frac{\partial t_2^*}{\partial r} + (\mu_n^2 + \nu_m^2)t_2^* = F^*(t_1)\,, \tag{23}$$

where

$$F_0^* = \frac{1}{C_m C_n}\int_0^R\int_0^L F_0 \cos(\mu_n z) rJ_0(\nu_m z)drdz\,, \tag{24}$$

$$F^*(t_1) = \frac{1}{C_m C_n}\int_0^R\int_0^L F(t_1)\cos(\mu_n z) rJ_0(\nu_m z)drdz\,. \tag{25}$$

Solving equations (22) and (23) in view of the transformed entry conditions, we obtain:

$$t_1^* = \exp\left[(\mu_n^2 + \nu_m^2)\alpha_0\tau\right]\left\{t_0^* + \int_0^\tau F_0^* \exp\left[(\mu_n^2 + \nu_m^2)\alpha_0\tau\right]d\tau\right\}, \tag{26}$$

$$t_2^* = \exp\left[(\mu_n^2 + \nu_m^2)\alpha_0\tau\right]\left\{t_0^* + \int_0^\tau F^*(t_1) \exp\left[(\mu_n^2 + \nu_m^2)\alpha_0\tau\right]d\tau\right\}, \tag{27}$$

where

$$t_0^* = \frac{t_0 R}{\mu_n \nu_m C_m C_n} \sin(\mu_n L) J_1(\nu_m R)\,. \tag{28}$$

Making inverse transformations, we discover:

$$t_1 = \sum_m \sum_n \exp\left[(\mu_n^2 + \nu_m^2)\alpha_0 \tau\right] \left\{ \frac{t_0 R}{\mu_n \nu_m C_m C_n} \sin(\mu_n L) J_1(\nu_m R) + \right.$$
$$\left. + \int_0^\tau F_0^* \exp\left[(\mu_n^2 + \nu_m^2)\alpha_0 \tau\right] d\tau \right\} \cos(\mu_n z) J_0(\nu_m r). \tag{29}$$

$$t_2 = \sum_m \sum_n \exp\left[(\mu_n^2 + \nu_m^2)\alpha_0 \tau\right] \left\{ \frac{t_0 R}{\mu_n \nu_m C_m C_n} \sin(\mu_n L) J_1(\nu_m R) + \right.$$
$$\left. + \int_0^\tau F^*(t_1) \exp\left[(\mu_n^2 + \nu_m^2)\alpha_0 \tau\right] d\tau \right\} \cos(\mu_n z) J_0(\nu_m r). \tag{30}$$

References

[1] Koshlyakov N.S., Gliner E.B. and Smirnov M.M. (1970) *Equations of Mathematical Physics in Partial Derivatives.* Nauka, Moscow

[2] Bogoljubov N. and Mitropolsky Yu. (1961) *Asymptotic Methods in the Theory of Nonlinear Oscillation.* Hindustan Publishing Corp., Dehli

[3] Aizen A.M. (1970) Solution of Nonlinear Heat Conduction Problems by the Combined method of perturbations and finite integral transformations. *Journal of Engineering Physics and Thermophysics* **19** (5), 945-947

[4] Fedotkin I.M. and Aizen A.M. (1975) *Asymptotic Methods in the Heat and Mass Transfer Problems.* Vyscha Shkola, Kiew *(in Russian)*

Received on the 17th of April 2004

Computer Modelling & New Technologies, 2004, Volume 8, No.1, 24-38
Transport and Telecommunication Institute, Lomonosov Str.1, Riga, LV-1019, Latvia

MATHEMATICAL MODELS WITH APPLICATION OF STATISTICAL INFORMATION IN TRANSPORTATION MANAGEMENT PROCESS

A. BAUBLYS

Transport Research Institute, Vilnius Gediminas Technical University,
Plytines 27, LT–2040, Lithuania,
E-mail: abaublys@takas.lt

In the course of freight transportation its technological process is influenced by lots of random factors. Classification of random factors in the whole hierarchical structure of the technological transportation process is presented, together with the assessment of the dependence of separate random factors. Statistical information on freight and transport flows is renewed and replenished in the course of time. With the growth of information amounts the costs of its storage increase as well. Therefore the relevant algorithms for obtaining required statistical assessments with the least statistical information are presented in the article. It is deduced that in the modelling of transport networks and freights as well as the flows of transport means in them, it is analytically proper to describe random factors by the non-parametric assessment.
Keywords: *freight transportation, mathematical modelling*

1. Introduction

It is necessary to assess aiming at a successful freight transportation the factors influencing the transportation time, quality and amount of the freight transported. At first sight it seems that various random factors are constantly affecting a strictly regulated process of transportation. Transportation process efficiency may decrease considerably without assessing these factors by the determined models for planning and management.

Basing on the analysis of the world-wide known transport science magazines of the last 20 years, such as *"TRANSPORTATION SCIENCE"*, *"TRANSPORT THEORY AND STATISTICAL PHYSICS"*, *"TRANSPORTATION RESEARCH PART B – METHODOLOGICAL"* I have noticed, that in this field it is suggested to use statistical probability models. However, there are no articles about the random factors themselves, about their formation, classification, about the mathematical models necessary for the accumulation of statistical information in such a way that it should not be stored too long, so that having prior assessments of these factors and having supplemented them with a new statistical information – automatically new assessments of the random factors would be attained.

2. Random Factors and their Classification

Random factors have to be classified within the whole hierarchic structure of the technological transportation process. Such structure should comprise freight suppliers and receivers, transport operators and forwarders, terminals with their technological processes, natural conditions, roads, i.e. everything that directly or indirectly influences the formation of random factors. Random factors may emerge because of subjective as well as objective reasons.

Objective reasons may be divided into three groups: technical, organisational and economical. The main technical reasons are as follows: the condition of industrial basis of the transportation process (transport means, containers, lifting means, etc.) and the technological level of operations. Organisational reasons – specialisation, scientific-technical information, means enhancing the quality of transportation, operation of customs and their subdivisions, moral responsibility for the quality of work, etc. Economical reasons – tariffs, forms and levels of pay, work consumption, material incentives, etc.

Main subjective reasons include professional, general and cultural level of employees, emotional and psychological features of their characters, the adequacy of personal and public interests, their personal interest in the results of their work.

Let us discuss in more detail the scheme of random factors' impact on the transportation quality. A team and operator should be interested in the quality of transportation: forming freight transport consignment, preparing documentation, packaging and handling freight during its transportation, etc. One of the regularities of random factors' formation is the fact that the errors made in the earlier stage of transportation pass to the next stage. Effective and precise information in all stages facilitates the elimination of random factors. The present classification of reasons of random factors' occurrence does not pretend to be absolutely comprehensive, however, in our opinion it demonstrates the complexity of the phenomena finally determining the efficiency of technological processes of transportation.

Formation and occurrence of random factors in the technological process of transportation is observed in the following stages: 1) scientific research work; 2) selection of the types of transportation; 3) f ormation of freight consignment; 4) determination of transportation routes; 5) freight handling/loading; 6) technological processes in terminals; 7) process of transportation (natural conditions, roads, etc.) 8) operation of customs. Reiterative random factors may occur because of various reasons, for instance, one of them might be an accident during transportation, the reasons of which also may vary: driver's fault, disorderly transport means, inaccurate loading/handling, roads technical conditions, meteorological conditions, etc.

Generally the technical-economical indices of transportation process should be analysed as random factors, which in turn are random for every meaning of reason as well. The reasons are as follows: the time or other parameters of the technological transportation process. Thus the optimal criteria should also be considered as random, not determined.

Majority of indices defining the assessment of the technological transportation process are closely interconnected; therefore it has to be taken into account when these indices are used as the criteria of optimality. For the definition of the digital characteristics of technical-economical indices according to the statistical information, obtained in the technological transportation process, the assessment of mathematical probability, correlation and dispersion functions should be calculated.

3. Assessment of Interdependency of Different Random Factors

Different variable parameters in the beginning of the transportation process will be indicated by $X_1, X_2, ..., X_n$; parameters determining the transportation process in progress will be indicated by $Z_1, Z_2, ..., Z_m$, and variable parameters of the exit from the transportation process will be indicated by $Y_1, Y_2, ..., Y_s$ (Figure 1). Then initial random quantities marked by $X_1, X_2, ..., X_n$ will be analysed as components of the random vector *X*, the random quantities $Z_1, Z_2, ..., Z_m$ – as components of the random vector *Z* and the exit random quantities $Y_1, Y_2, ..., Y_s$ – as components of the random vector *Y*.

It is not possible to make only the analysis of separate initial and variable factors, characterising the quality of transportation process in progress, because they are insufficient for obtaining comprehensive characteristics of the technical-economical indices of the transportation process as well as it is impossible to define the optimal variant of the transportation process management. The transportation process should be analysed as a multi-measurable process with a large number of initial parameters, the general assessment of which allows a complex evaluation of the efficiency of functioning of the technological transportation process.

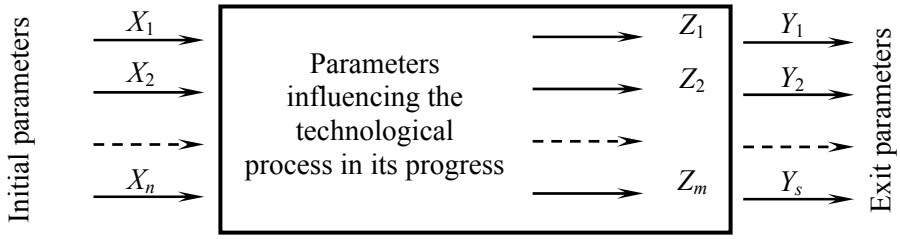

Figure 1. Scheme of the technological transportation process

It is obvious that according to the characteristics of the multi-measurable process, the meanings of every exit variable *Y* should be defined. Whereas the exit variables of the multi-measurable process may be independent, correlated or connected by the functional interdependence. Practically the characteristics

of the transportation process should be analysed in each of the aforesaid cases. At the beginning we shall analyse the characteristics of the transportation process, when the initial variable quantities are interdependent $Y_1, Y_2, ..., Y_s$.

Let us presume that general probability density of the vectored random quantities *X*, *Z* and *Y* is normal

$$\varphi_t(U_1, ..., U_t) = \frac{1}{\sigma_{u_1}, ..., \sigma_{u_t}\sqrt{(2\Pi)^t E}} \times \exp\left\{\frac{-1}{2E}\sum_{\mu,\, v=1}^{t} E_{\mu,\, v}\left(\frac{U_\mu - M\{U_\mu\}}{\sigma_{u\mu}}\right)\left(\frac{U_v - M\{U_v\}}{\sigma_{uv}}\right)\right\}, \quad (1)$$

here, for the abridgement's sake there is introduced the random vector quantity *U* which is made of $X_1, ..., X_n$, $Z_1, ..., Z_m$, $Y_1, ..., Y_s$; $t = n + m + s$; E – determinant of series t.

$$E = \begin{vmatrix} 1 & \rho_{u_1u_2} & ... & \rho_{u_1u_t} \\ \rho_{u_2u_1} & 1 & ... & \rho_{u_2u_t} \\ ... & ... & ... & ... \\ \rho_{u+u_1} & \rho_{u+u_2} & ... & 1 \end{vmatrix}, \quad (2)$$

or *X*, *Z*, *Y* in the variables' marking

$$E = \begin{vmatrix} 1 & \rho_{x_1x_2} & ... & \rho_{x_1x_n} & \rho_{x_1z_1} & ... & \rho_{x_1z_m} & \rho_{x_1y_1} & ... & \rho_{x_1y_s} \\ \rho_{x_nx_1} & \rho_{x_nx_2} & ... & 1 & \rho_{x_nz_1} & ... & \rho_{x_nz_m} & \rho_{x_ny_1} & ... & \rho_{x_ny_s} \\ \rho_{z_1x_1} & \rho_{z_1x_2} & ... & \rho_{z_1x_n} & 1 & ... & \rho_{z_1z_m} & \rho_{z_1y_1} & ... & \rho_{z_1y_s} \\ ... & ... & ... & ... & ... & ... & ... & ... & ... & ... \\ \rho_{z_nx_1} & \rho_{z_mx_2} & ... & \rho_{z_mx_n} & \rho_{z_mz_1} & ... & 1 & \rho_{z_my_1} & ... & \rho_{z_my_s} \\ \rho_{y_1x_1} & \rho_{y_1x_2} & ... & \rho_{y_1x_n} & \rho_{y_1z_1} & ... & \rho_{y_1z_m} & 1 & ... & \rho_{y_1y_s} \\ ... & ... & ... & ... & ... & ... & ... & ... & ... & ... \\ \rho_{y_sx_1} & \rho_{y_sx_s} & ... & \rho_{y_sx_n} & \rho_{y_sz_1} & ... & \rho_{y_sz_m} & \rho_{y_sy_1} & ... & 1 \end{vmatrix};$$

$E_{\mu v}$ is an algebraic supplement ρ_{umnv} in the determinant (2).

For the analysis of the case when the exit variables are independent, it is necessary to determine characteristics of every variable $Y_k\,(k = 1, 2, ..., s)$ as well as the influence exercised on them by the initial variables *X* and the variables *Z*, characterising the inner state of the process. Let us indicate the general probabilities' *X*, *Z* and *Y* density $Y_{n+m+1}(Y_k, X_1, ..., X_n, Z_1, ..., Z_m)$, whereas the random vectored quantities' *X* and *Z* by the general probability density $\varphi_{n+m}(X_1, ..., X_n, Z_1, ..., Z_m)$. The probability densities $\varphi_{n+m+1}(\varphi_k, X_1, ..., X_n, Z_1, ..., Z_m)$ and $\varphi_{n+m}(X_1, ..., X_n, Z_1, ..., Z_m)$ are not zero ones and they correspond to the equation (1) with determinants' σ and *F* meanings correspondingly of $(n + m + 1)$ and $(n + m)$ series

$$\sigma = \begin{vmatrix} 1 & \rho_{x_1x_2} & ... & \rho_{x_1z_m} & \rho_{x_1y_k} \\ \rho_{x_2x_1} & 1 & ... & \rho_{x_2z_m} & \rho_{x_2y_k} \\ ... & ... & ... & ... & ... \\ \rho_{z_mx_1} & \rho_{z_mx_2} & ... & 1 & \rho_{z_my_k} \\ \rho_{y_kx_1} & \rho_{y_kx_2} & ... & \rho_{y_kz_m} & 1 \end{vmatrix}; \quad (3)$$

$$F=\begin{vmatrix} 1 & \rho_{x_1x_2} & \dots & \rho_{x_1x_n} & \rho_{x_1z_1} & \dots & \rho_{x_1z_m} \\ \dots & \dots & \dots & \dots & \dots & \dots & \dots \\ \rho_{x_nx_1} & \rho_{x_nx_2} & \dots & 1 & \rho_{x_nz_1} & \dots & \rho_{x_nz_m} \\ \rho_{z_1x_1} & \rho_{z_1x_2} & \dots & \rho_{z_1x_n} & 1 & \dots & \rho_{z_1z_m} \\ \dots & \dots & \dots & \dots & \dots & \dots & \dots \\ \rho_{z_mx_1} & \rho_{z_mx_2} & \dots & \rho_{z_mx_n} & \rho_{z_mz_1} & \dots & 1 \end{vmatrix}. \quad (4)$$

General characteristic of the technological transportation process is a conditional probability density $\varphi(Y_k/(X_1,...,X_n,Z_1,...,Z_m))$, according to which the meaning may be defined by the general characteristics of the prior variables X and the inner state variables Z by transformation of the distribution laws of these random quantities.

Generally, the conditional density $\varphi(Y_k/(X_1,...,X_n,Z_1,...,Z_m))$ is determined by the general probability densities $\varphi_{n+m+1}(Y_kX_1,...,X_n,Z_1,...,Z_m)$ and $\varphi_{n+m}(X_1,...,X_n,Z_1,...,Z_m)$:

$$\varphi(Y_k/(X_1,...,X_n,Z_1,...,Z_m))=\frac{\varphi_{n+m+1}(Y_k,X_1,...,X_n,Z_1,...,Z_m)}{\varphi_{n+m}(X_1,...,X_n,Z_1,...,Z_m)}. \quad (5)$$

If common probability densities $\varphi_{n+m}(X_1,...,X_n,Z_1,...,Z_m)$ and $\varphi_{n+m+1}(Y_k,X_1,...,X_n\ Z_1,...,Z_m)$ are normal, then for the analysed case the conditional probability density

$$\varphi(Y_k/(X_1,...,X_n,Z_1,...,Z_m))=\frac{1}{\sqrt{2\pi}\sigma_{yk}}\sqrt{\frac{F}{\sigma}}\exp\left\{\frac{1}{2F}\sum_{k,l=1}^{n+m}F_{kl}\times\right.$$

$$\left.\times\left(\frac{\nu_k-M\{\nu_k\}}{\sigma_{\nu_k}}\right)\left(\frac{\nu_t-M\{\nu_l\}}{\sigma_{\nu_l}}\right)-\frac{1}{2\sigma}\sum_{m,\nu=1}^{n+m+1}\sigma_{\mu_\nu}\times\left(\frac{U_\mu-M\{U_\mu\}}{\sigma_{u\mu}}\right)\left(\frac{U_\nu-M\{U_\nu\}}{\sigma_{u\nu}}\right)\right\},$$

here $F_{k,l}$ – of element $\rho_{k,l}$ algebraic supplement in the determinant (4); $\sigma_{\mu,\nu}$ – element $\rho_{m,\nu}$ algebraic supplement in the determinant (3) $\nu(X_1,...,X_n,\ Z_1,...,Z_m)$, $U(Y_k,X_1,...,X_n,Z_1,...,Z_m)$. Given the conditional density $\varphi(Y_k/(X_1,...,X_n,Z_1,...,Z_m))$ for the definition of characteristics X and Z general characteristics of the exit variable Y, i.e. the probability density $\varphi_{yk}(Y_k)$ is defined by of the following integral equation:

$$\varphi_{yk}(Y_k)=\int_{-\infty}^{\infty}\dots\int_{-\infty}^{\infty}\varphi(Y_k/(X_1,...,X_n,Z_1,...,Z_m))\varphi_{n+m}(X_1,...,X_n,Z_1,...,Z_m)dX_1,...,dX_n,dZ_1,...,dZ_m.$$

While knowing general characteristics $\varphi(Y_k/(X_1,...,X_n,Z_1,...,Z_m))$, we may also define the main digital characteristics of X and Z in the aspect of the exit variable Y_k, i.e. the conditional mathematical probability and conditional dispersion

$$M\{Y_k/(X_1,...,X_n,Z_1,...,Z_m)\}=\frac{\int_{-\infty}^{\infty}Y_k\varphi_{n+m+1}(Y_k,X_1,...,X_n,Z_1,...,Z_m)dy_k}{\int_{-\infty}^{\infty}\varphi_{n+m+1}(Y_k,X_1,...,X_n,Z_1,...,Z_m)dy_k}=$$

$$=\int_{-\infty}^{\infty}Y_k\frac{\varphi_{n+m+1}(Y_k,X_1,...,X_n,Z_1,...,Z_m)}{\varphi_{n+m}(X_1,...,X_n,Z_1,...,Z_m)};$$

thus, we shall assess the equation (5) and obtain

$$M\{Y_k/(X_1,...,X_n,Z_1,...,Z_m)\}=\int_{-\infty}^{\infty}Y_k\varphi\left(Y_k/(X_1,...,X_n,Z_1,...,Z_m)\right)dy_k\ .$$

Whereas the conditional dispersion Y_k in the aspect of X and Z

$$D\{Y_k/(X_1,...,X_n,Z_1,...,Z_m)\}=\int_{-\infty}^{\infty}\left[Y_k-M\{Y_k/(X_1,...,X_n,Z_1,...,Z_m)\}\right]^2\times$$
$$\times\varphi\left(Y_k/(X_1,...,X_n,Z_1,...,Z_m)\right)dy_k\ .$$

Thus, while defining the characteristics of the technological transportation process, when the random factors are assessed, it is necessary to determine the unconditional and conditional dispersion laws. The constant accumulation of statistic information is necessary for this reason.

It is often expedient to use digital characteristics instead of the random factors' distribution laws for practical purposes. Although the digital characteristics give insufficient information on random factors, however, for the solution of certain transportation issues they fully suffice, and their determination is by far easier. A complete analysis and synthesis of the characteristics of the transportation processes is carried out according to the general characteristics, i.e. according to the unconditional and conditional distribution laws. These laws may be employed for the definition of different characteristics of the technological transportation processes. However, as the presented formula shows, the characteristics of the technological transportation processes may be determined in such cases when the general laws of random quantities' distribution are known. This condition must be observed in the designing of systems for accumulation and processing of statistical information. If the exit variables are correlated, then for the management of the technological transportation process there may be used the characteristics of one or several exit variables.

4. Accumulation of Statistical Information on the Transportation Process

4.1. NON-PARAMETRICAL ASSESSMENT OF DISTRIBUTION DENSITY

In the modelling of transport networks and the flows of freight and transport means, the analytical description of the density distribution of their random factors is carried out by parametric assessments. In certain issues the distribution type of analysed factors' density in the course of time is altering (new nomenclature of consignment, shifting to other working conditions, etc.), therefore the distribution description by the law of a selected type is inaccurate and absolutely impossible (from the point of view of calculation). Besides, the approximation of empirical distributions by using parametric assessments is very sensitive to data errors. Even one mistake made during the introduction of the prior information $x_1,...,x_N$ into the computer, may exercise such a great effect on the meanings of sampling moments that the analytical description of the curves will be very inexact. Unlike the parametric – the non-parametric assessment of density distribution has a number of merits. Firstly, when in the course of time the type of flows distribution density is changing, it is possible to approximate by the exactness sufficient enough for practical use. Secondly, this assessment is by far less sensitive to data errors.

In the case of non-parametric assessment it may be written

$$f(x)=\frac{1}{N}\sum_{i=1}^{N}\frac{1}{\sqrt{2\pi}\lambda}e^{-(x-x_i)^2/2\lambda^2}\ , \qquad (6)$$

here λ is the coefficient of equalisation.

Since in the given assessment we have to remember all sample realisations $x_1,...,x_N$, we may use the following assessment

$$f(x) = -\frac{1}{\sqrt{2\pi}\lambda} e^{-y^2/2\lambda^2} \sum_{j=1}^{t} C_j y_j \,, \tag{7}$$

here the coefficients C_j are defined by the formula

$$C_j = \frac{1}{j!(\lambda)^{2j}} \frac{1}{N} \sum_{i=1}^{N} y_i^j e^{-y_i^2/2\lambda^2} \,, \tag{8}$$

here $y = x - \Delta$; $y_i = x_i - \Delta$, and the coefficient Δ equals approximately to the mathematical probability of distribution.

In the phenomenon (7) the members' number t is found by experimental way. Since even because of very "curved" distributions and very inaccurate data the densities calculated according to the (7) by using four members coincide, so further we shall presume that because of the (7) $t = 4$. Non-parametric assessment of such type requires remembering only of the coefficients λ, Δ, C_0, C_1, …, C_t, i.e. the $t + 3$ parameters, that simplifies the solution of the work on the problem.

Selection of equalisation coefficients. Non-parametric dispersion assessment includes the equalisation coefficient λ, the optimal meaning of which is determined by the distribution dispersion and sample size: the larger dispersion and the smaller is the sample, the larger is λ. If the λ is very small, then even in case of a very large sample the non-parametric assessment will be very sensitive and consequently imprecise, otherwise the unevenness of the distribution density profile will not be assessed.

Let us analyse a case when the distribution density

$$f(x) = \sum_{i=1}^{k} P_i \frac{1}{\sqrt{2\pi}\sigma_i} e^{-(x-\sigma_t)^2/2\sigma_t^2} \,. \tag{9}$$

The latter formula practically allows a good approximation of most observed distributions in freight flows' research.

We shall apply the approximation quality criterion for selection of an optimal equalisation parameter.

$$U = \frac{1}{Q} \int_{-\infty}^{\infty} E_x \left[f_N(x) - f(x) \right]^2 dx \tag{10}$$

here the E_x – is the mathematical probability of the quantity N, $Q = \int_{-\infty}^{\infty} f^2(x)\,dx$. After having indicated

$$\frac{1}{\sqrt{2\pi}a} e^{-(x_i-b)^2/2a^2} = N\left(x, b, a^2\right), \tag{11}$$

the expressions (6) and (9) will be written

$$f_N(x) = \frac{1}{N} \sum_{i=1}^{N} \left(x, x_{i,} \lambda^2 \right), \tag{12}$$

$$f(x) = \sum_{j=1}^{k} P_j N\left(x, \mu_j, \sigma_j^2 \right). \tag{13}$$

We should take into account while calculating the (10), that

$$\int_{-\infty}^{\infty} N(x,\ a_1 b_1) N(x, a_2, b_2)\,dx = N(a_1, a_2, b_1 + b_2), \tag{14}$$

$$\int_{-\infty}^{\infty}\left[N^2\left(x,a_1,b_1\right)\right]^2 N\left(x,a_2,b_2\right)dx=\sqrt{\frac{2b_2+b_1}{a}}\left[N\left(a_1,a_2,2b_2+b_1\right)\right]. \tag{15}$$

Thus we obtain

$$E_x\left[f_N(x)-f(x)\right]^2=E_x\left|f_N(x)\right]^2-2E_x f_N(x)f(x)+f^2(x), \tag{16}$$

$$E_x f_N(x)=\frac{1}{N}\sum_{i=1}^{N}\int_{-\infty}^{\infty}\ldots\int_{-\infty}^{\infty}N\left(x,x_i,\lambda^2\right)\prod_{i=1}^{N}f\left(x_i\right)dx_1,\ldots,dx_N\ . \tag{17}$$

Since

$$\int_{-\infty}^{\infty}f\left(x_i\right)dx_i=1,$$

the expression (17) may be written in the following way

$$E_x f_N(x)=\sum_{s=1}^{k}P_s N\left(x,\mu_s,\lambda^2+\sigma_s^2\right). \tag{18}$$

Further we calculate the following

$$E_x\left[f_N(x)\right]^2=\frac{1}{N}\sum_{s=1}^{k}\left[P_s\sqrt{\frac{2\sigma_s^2+\lambda^2}{\lambda^2}}N\left(x,\mu_s;2\sigma_s^2+\lambda^2\right)+\left(1-\frac{1}{N}\right)\sum_{s=1}^{k}P_s N\left(x,\mu_s,\sigma_s^2+\lambda^2\right)\right]^2. \tag{19}$$

After putting the (19) and (18) into (16) and (10), and afterwards applying the equation (14) we shall obtain

$$U=\left[\frac{1}{N}\sum_{s=1}^{k}P_s\sqrt{\frac{\lambda^2+2\sigma_s^2}{\lambda}}N\left(\mu_s,\mu,4\sigma_s^2+2\lambda\right)^2+\left(1-\frac{1}{N}\right)\sum_{s,l=1}^{k}P_s P_l,N\left(\mu_s,\mu_l,\sigma_s^2+\sigma_l^2+2\lambda^2\right)-\right.$$
$$\left.-2\sum_{s,l=1}^{k}P_s P_l,N\left(\mu_s,\mu_l,\sigma_s^2+\sigma_l^2+\lambda^2\right)+\sum_{s,l=1}^{k}P_s P_l,N\left(\mu_s,\mu_l,\sigma_s^2+\sigma_l^2\right)\right]/Q\ , \tag{20}$$

here

$$Q=\sum_{s,l=1}^{k}P_s P_l N\left(\mu_s,\mu_l,\sigma_s^2+\sigma_l^2\right).$$

The latter (20) expression enables the finding of optimal meaning λ for the distribution described in the formula (9). Unknown parameters are included in this formula. Presuming that the k is set (practically good results are obtained when $k=3\div5$), the parameters P_i, μ_i, σ_i may be found by the way of the iterative procedures.

The algorithm of assessments' finding is formed by the following steps:

1) we set $P_1^{(1)},\ldots,P_k^{(1)},\mu_1^{(1)},\ldots,\mu_k^{(1)},\sigma_1^{(1)},\ldots,\sigma_k^{(1)}$;
2) we calculate

$$\alpha_{ij}^{(t)}=\frac{P_j^{(t-1}N\left(x_i,\mu_j,\sigma_j^{(t-1)}\right)}{\sum_{j=1}^{k}P_j^{(t-1)}N\left(x_i,\mu_j^{(t-1)},\sigma_j^{(t\text{-}1)}\right)},\ i,j=1,\ \ldots,N;$$

3) we obtain new meanings $P_1^{(t)},...,P_k^{(t)},\mu_1^{(t)},...,\mu_k^{(t)},\sigma_1^{(t)},...,\sigma_k^{(t)}$ according to the formulae

$$P_j^{(t)} = \frac{\sum_{i=1}^{N} \alpha_{ij}^{(t)}}{N},$$

$$\mu_j^{(t)} = \frac{\sum_{i=1}^{N} \alpha_{ij}^{(t)} x_i}{\sum_{i=1}^{N} \alpha_{ij}^{(t)}} = \frac{\sum_{i=1}^{N} \alpha_{ij}^{(t)} x_i}{P_j^{(t)} N},$$

$$\sigma_j^{(t)} = \frac{\sum_{i=1}^{N} \alpha_{ij}^{(t)} \left(x_i - \mu_j^{(t)}\right)^2}{P_j^{(t)} N}.$$

We repeat the process starting from the second step until the meanings P_i, μ_i, σ_i will vary within narrow limits, i.e. until we reach the desired precision.

TABLE 1. Results of experimental calculations for the coefficient of optimal equalisation

Sample number	Quantity of the sample N	Optimisation according to the formula (20)	
		$\lambda_{opt.}$	$U_{\min}$
1	40	0,844	0,0472
2	140	0,623	0,0199
3	40	0,858	0,04655
4	40	0,709	0,0623
5	113	0,551	0,0297
6	40	1,293	0,0679
7	181	0,894	0,0230
8	40	0,867	0,0586
9	131	0,656	0,0258

Experimental calculations were carried out, i.e. according to the above formulae there were calculated the coefficients $\mu_1,...,\mu_k,\sigma_1,...,\sigma_k,P_1,...,P_k$ included into the (9) and with the help of minimisation of the (20) the optimal meanings of the equalisation coefficient $\lambda_{opt.}$ were obtained, as well as there was defined the meaning of $U_{\min}$ corresponding to the $\lambda_{opt.}$. The results of the experiment are presented in the Table 1, which shows that using the formula obtained by us (9) the correctness of approximation of density of random quantities is significantly more precise, the equalisation parameter defined according to the (20) is 1,2–2 times less than in the case of normal distribution. That is why it is expedient to use the formula (9) for the optimisation of the parameter λ and for the description statistical data of freight flows.

4.2. MATHEMATICAL MODELS IN ACCUMULATION OF STATISTICAL INFORMATION

Statistical information on the freight and transport flows is renewed and replenished in due course. With the growth of the amount of information the costs of its storage are increasing too. Therefore, our aim is to obtain necessary statistical assessments with the minimal amount of statistical information.

The assessment of distribution of random factors by the Bayesian method. Presumably we have a sample X, made of N meanings $x_1,...,x_N$. Considering the meanings x as random quantities we shall assess distribution function of the random quantity X. For an analytical description of the distribution X, there is necessary a relevant prior information on the distribution type. Let us presume that it is known,

i.e. there is known the parametric probabilities' density $f(X/\theta)$, here $\theta = \begin{pmatrix} \theta_1 \\ \theta_2 \\ \vdots \\ \theta_r \end{pmatrix}$ – vector of the parameters describing the distribution of the random quantity *x*; the *r* – is the number of parameters and presumably known the prior distribution of the vector's parameters $\theta f_{apr.}(\theta)$, the latter may be defined by an experimental assessment. Then the *X* distribution may be assessed with the help of the Bayesian formula [1].

At the beginning we shall obtain the aposterioric density of distribution of the vector's parameters. Considering that observations in the sample $x_1, ..., x_N$ are independent, according to the Bayesian formula it is as follows

$$f(\theta / x_1, ..., x_N) = \frac{\prod_{i=1}^{N} f(x_i / \theta) f_{apr.}(\theta)}{\int_{\Omega_\theta} \prod_{i=1}^{N} f(x_i / \theta) f_{apr.}(\theta) d\theta}, \tag{21}$$

here the integration is in r – measurable area Ω_θ by changing the parameter θ. The aposterioric distribution of X is obtained by integrating

$$f(X / x_1, ..., x_N) = \int_{\Omega_\theta} f(X/\theta) f(\theta / x_1, ..., x_N) d\theta . \tag{22}$$

By putting the (21) into (22) we obtain

$$f(X / x_1, ..., x_N) = \frac{\int_{\Omega_\theta} f(X/\theta) \prod_{i=1}^{N} f(x_i / \theta) f_{apr.}(\theta) d\theta}{\int_{\Omega_\theta} \prod_{i=1}^{N} f(x_i / \theta) f_{apr.}(\theta) d\theta} .$$

After the new sample of the phenomena $x_{n+1}, ..., x_{n+m}$ is obtained and it is necessary to specify the distribution $f(X)$ by using new data, then instead of the prior distribution $f_{apr.}(\theta)$ we shall use the former prior one $f(\theta / x_1, ..., x_N)$. Let us notice that such method does not require the storage of all the meanings of a sample; only the meanings of the aposterioric distribution $f(\theta / x_1, ..., x_N)$ are subject to storage, namely – only a certain number of coefficients characterising it. At the beginning of the data accumulation process we may not have the $f_{apr.}$ on the whole, then the Bayesian postulate is applied and the prior distribution is considered uniform [1].

The presented formulae would lose their practical importance if they would not have concrete distribution types $f(X/\theta)$ and $f_{apr.}(\theta)$. Besides, it is preferable that the analytical type of the prior and aposterioric density would be uniform, because then the calculation algorithms and programmes become simpler.

Normal distribution. Let us analyse the case when random qualities are distributed according to the normal law, the density of which is

$$f(X / \mu, \sigma) = \frac{1}{\sqrt{2\pi}\sigma} \exp\left[-\frac{1}{2} \frac{(x-\mu)^2}{\sigma^2} \right]. \tag{23}$$

In the given case the parameters' vector $\theta = \begin{pmatrix} \mu \\ \sigma \end{pmatrix}$, and

$$f(x_1,...,x_N/\mu,\sigma)=C_0\sigma^{-N}\exp\left(-\frac{1}{2}\frac{S(N-1)}{\sigma^2}\right)\exp\left(-\frac{1}{2}\frac{N(\bar{x}-\mu^2)}{\sigma^2}\right), \quad (24)$$

here $\bar{x}=\frac{1}{N}\sum_{i=1}^{N}x_i$; $S=\frac{1}{N-1}\sum_{i=1}^{N}(x_i-\bar{x})^2$ – the sample medium and dispersion accordingly $C_0=(2\pi)^{-N/2}$.

The prior distribution of parameters μ and σ is selected so that its density would be analogous to the density of the conditional density

$$f(\mu,\sigma)=C_1\sigma^{-n}\exp\left[-\frac{1}{2}\frac{a(n-1)+n(\mu+\mu_0)^2}{\sigma^2}\right]. \quad (25)$$

The coefficient C_1 depends on n and may be obtained from the rationing condition. The coefficient C_1 is not calculated here, because it does not depend on μ and σ. After putting the (25) into (21), and after a corresponding rearrangement, we shall obtain

$$f(\sigma,\mu/x_1,...,x_N)=\frac{1}{C_3}\sigma^{-N*}\exp\left[-\frac{1}{2}\frac{(N^*-1)a^*+N^*(\mu-\mu^*)}{\sigma^2}\right], \quad (26)$$

here C_3 is obtained from the rationing condition; $N^*=N+n$;

$$a^*=S\frac{N-1}{N+n-1}+a\frac{n-1}{N+n-1}+\frac{Nn(\mu_0-\bar{x})^2}{(N+n)[(N+n)-1]}; \quad (27)$$

$$\mu^*=\bar{x}\frac{N}{N+n}+\mu_0\frac{n}{N+n}. \quad (28)$$

Now let us calculate the coefficient C_3.

Having noticed, that $\frac{1}{\sqrt{2\pi}\sigma/\sqrt{N^*}}\int_{-\infty}^{\infty}\exp\left(-\frac{1}{2}\frac{(\mu-\mu^*)^2}{\sigma^2/N^*}\right)d\mu=1$,

after the relevant rearrangements $C_3=\frac{1}{2}\sqrt{\frac{2\pi}{N^*}}\left[\frac{a^*(N^*-1)}{2}\right]^{(N^*-2)/2}\Gamma\left(\frac{N^*-2}{2}\right)$.

Thus the aposterioric distribution of the parameters σ and μ

$$f(\sigma,\mu/x_1,...,x_N)=\frac{\sigma^{-N^*}\exp\left[-\frac{1}{2}\frac{(N^*-1)a^*+N^*(\mu-\mu^*)^2}{\sigma^2}\right]}{\sqrt{\frac{\pi}{2N^*}}\left[\frac{a^*}{2}(N^*-1)\right]^{(N^*-2)/2}\Gamma\left(\frac{N^*-2}{2}\right)}. \quad (29)$$

The aposterioric density of the *x* distribution

$$f(X/x_1,...,x_N)=\frac{\Gamma\left(\frac{N^*-1}{2}\right)}{\sqrt{2\pi}\Gamma\left(\frac{N^*-2}{2}\right)\sqrt{\frac{a^*(N^*-1)}{2}}}\left[1+\frac{N^*(X-\mu^*)^2}{(N^{*2}-1)a^*}\right]^{-(N^*-1)/2}. \quad (30)$$

The aposterioric density may be approximated by the normal one (23) by putting instead of the σ and μ more probable meanings obtained from (29). By differentiation we obtain the following more expected meanings of the parameters $\mu=\mu^*$, $\hat{\sigma}^2=a^*$. Then the aposterioric density is approximated by the phenomenon

$$f(X/\hat{\mu},\hat{\sigma})=\frac{1}{\sqrt{2\pi}\hat{\sigma}}\exp\left[-\frac{1}{2}\frac{(X-\hat{\mu})^2}{\hat{\sigma}^2}\right]. \quad (31)$$

In the presence of large N (31), the (30) approximates the density with great precision. As the (30) and (31) include only parameters $N^*=N+n, a^*$ (or $\hat{\sigma}$), μ^* (or $\hat{\mu}$), then every aposterioric distribution may be very simply used as an aprioric one. For this purpose only the parameters are recalculated

$$N_i=N_{i-1}+N,$$

$$\hat{\mu}_i=\mu_{i-1}\frac{N_{i-1}}{N_{i-1}+N}+\frac{N}{N_{i-1}+N}\bar{x},$$

$$\hat{\sigma}^2=\hat{\sigma}_{i-1}^2\frac{N_{i-1}-1}{N+N_{i-1}-1}+S\frac{N}{N+N_{i-1}-1}+\frac{NN_i(\mu_i-\bar{x})^2}{N+N_i(N+N_{i-1})}.$$

Consequently suffice it to remember only three coefficients: N_{i-1}, μ_{i-1} and σ_{i-1}. To demonstrate under which given N it is possible to use the simple (31) instead of the complicated formula (30) let us analyse the following example.

The sample, having 100 random quantity meanings, characterising the quantity alteration of freight consignment brought to the terminal, was divided into 20 portions with 5 realisations each. The meanings of the parameters of the aprioric distribution are: $\mu_0=300$, $\sigma_0=10$, $N_0=1$. According to the first sample we calculated x and s^*, and further according to (27) and (28) a^* and μ^*. According to these parameters we have calculated the meanings of the aposterioric density by the precise formula (30) and the approximate formula (31). Further on we use the meanings a^* and μ^* as the parameters of aprioric distribution and we repeat the calculation procedure for the second, the third, etc., samples. The diagrams of the distribution density are presented in the Figure 2, where the continuous line shows the distribution obtained according to the (30), and the dotted line – those according to the (31).

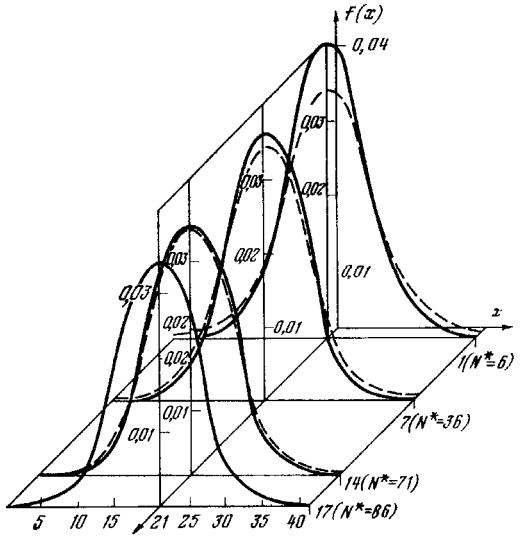

Figure 2. The diagrams of the distribution density

In the seventeenth interval the curves of the distribution density practically coincide completely. Already in the presence of $N = 70 - 85$ both density curves practically coincide and when the sample exceeds 100 it is possible to use much more simple (normal) density.

Logarithmic-normal distribution. As experiments have proved, by using logarithmic normal distribution

$$f(x) = \frac{1}{x\beta\sqrt{2\pi}} \exp\left(-\frac{\ln(x-a)^2}{2\beta^2} \right),$$

it is possible to introduce simplification without losing precision (sufficient for practice). Namely, if indicated $y = \ln x$, then random quantity y will be distributed according to the normal density

$$f(y) = \frac{1}{\sqrt{2\pi}\beta} \exp\left(-\frac{(y-a)^2}{2\beta^2} \right). \tag{32}$$

There may be occur difficulties in the interpretation of the results with (32), however during the calculation the simplicity of the formula (32) is very clear. For example, we need to calculate probability limits for x. Since y – monotharic function x, it is possible to define probability limits y: y_1 and y_2 (probability limits x: $x_1 = e^{y_1}$ and $x_1^{y_1}$).

The parameters a and β are correspondingly the medium and dispersion of the rearranged random quantity $y = \ln x$ and they are defined

$$a = \frac{1}{N}\sum_{i=1}^{N} y_i = \frac{1}{N}\sum_{i=1}^{n} \ln x_i \ , \tag{33}$$

$$\beta^2 = \frac{1}{N-1}\left(\sum_{i=1}^{n} (\ln x_i)^2 - a^2 \right). \tag{34}$$

Thus, the Bayesian model of normal distribution may be used for logarithmic normal distribution as well, after its relevant rearrangement.

Exponential distribution. This is characterised by one parameter $\hat{\lambda} = \frac{1}{N}\sum_{i=1}^{N} x_i$,

which is assessed according to a sample.

After obtaining of new data the meaning was corrected $\hat{\lambda}_n = \frac{\left(N\lambda_{c_i} + \sum_{i=1}^{N_N} x_i \right)}{N_N + N}$, here N – sample quantity according to which there were assessed earlier λ meanings; N_N – the amount of realisations obtained.

Non-parametric distribution. It was demonstrated earlier, that the optimal meaning of the equalisation coefficient $\lambda_{opt.}$ depends upon the sample quantity N. Therefore the coefficients C_j are the main function's λ, then, having obtained new information, the coefficient λ has to be changed and it is not possible to define the meanings of C_j by the formula (8). Therefore it has to be redone.

Since

$$e^x = 1 + \frac{x}{1!} + \frac{x^2}{2!} + \frac{x^3}{3!} + \ldots + \frac{x^n}{n!} + \ldots, \tag{35}$$

then (8) may be written in this way

$$C_j = \frac{1}{j!\lambda^2 j}\frac{1}{N}\sum_{i=1}^{N} y_i^j \left(1 - \frac{y_i^2}{2\lambda^2} + \frac{y_i^4}{2(2\lambda^2)^2} - \frac{y_i^6}{6(2\lambda^2)^3} + \ldots \right). \tag{36}$$

Limited by the first members of the line, we have

$$C_j = \frac{1}{j!\lambda^2 j}\frac{1}{N} y_i^j \sum_{s=0}^{k} \frac{(y_i)^{2s}(-1)^s}{s!2^s \lambda^{2s}}. \tag{37}$$

After changing the order of summing, we shall obtain

$$C_j = \frac{1}{j!}\sum_{s=0}^{k} \frac{(-1)^s}{s!2^s \lambda^{2(s+j)}} b_{2s+j}\ , \tag{38}$$

where $b_t = \frac{1}{N}\sum_{i=1}^{N}(y_i)^t$.

Thus, for the purpose of data accumulation (rehabilitation of the distribution densities) it is necessary to store $1+2k$ the coefficient b_t . After receiving new information it is necessary to obtain by the (20) the meaning of the optimal equalisation coefficient $\lambda_{opt.}$ for the new sample quantity, afterwards to recalculate the meaning b_t by the formula $b_{t_n} = \frac{N_s}{N_s + N_g} b_{t_s} + \frac{1}{N_s + N_g}\sum_{i=1}^{N_g} y_i^t$,

where b_{t_s} – the old meaning of the coefficient b_t , N_s – the sample quantity before the obtaining of new data, N_g – the quantity of obtained data. According to the calculated meanings $b_1, ..., b_{t+2k}$ and formulae (38) and (7) it is possible to obtain the assessment of distribution density.

In the course of calculation it is necessary to determine the degree of the polynomial (35). As it is apparent from (8), the sets to which $y_i / 2\lambda^2 > 8 \div 10$, practically will have no influence on the meaning of the coefficient C_j. Therefore the members, which $y_i > 20\lambda^2$, in calculation of the coefficients b_t , should be dismissed. Then in the line (36) the maximum member $\left[\frac{y_i^2}{2\lambda^2}\right]$ will not exceed 10. Thus, the k is obtained on condition that the member remaining in the line (36) is by far less than one, i.e.

$\frac{\left\{\left[\frac{y_i^2}{2\lambda^2}\right]_{\max}\right\}^k}{K!} << 1$. In the reality with $10^k / 10! \le 0{,}001$ we obtain $k \approx 30$.

The Weibull distribution. This is characterised by two parameters and its density

$$f(x) = \frac{mt^{m-1}}{x_0}\exp\left[-\left(\frac{t}{x_0}\right)^m\right],\ t \ge 0,\ m>0,\ x_0>0,$$

where m – the parameter of form; x_0 – the parameter of scale. This distribution is used in the research of reliability of transport and loading means, in description of failures' probability (breakdown).

Let us presume that during a certain time we analyse the n amount of transport means, and during the time r, $1 \le r \le n$, transport means failed – broke down, got out of order. The time of failure will be defined $t_1, ..., t_r$. This data may be used in calculation of the Weibull distribution parameters m and x_0 .

The latter parameters may also be defined by the method of maximum similarity; for this purpose it is necessary to solve the non-linear equations $x = \frac{1}{r}\left[\sum_{i=1}^{r} x_i^m + (n-r)x_r^m\right]$, $x = \frac{\sum_{i=1}^{r} x_i^m \ln x_i + (n-r)x_r^m \ln x_r}{\frac{r}{m} + \sum_{i=1} \ln x_i}$.

Since into the statistics $\sum t_i^m, \sum t_i^m \ln t_i$ there is included an unknown parameter m, the whole sample should be used in the calculations, for which cause the storage of not only certain but of all realisations is necessary.

Accumulation of data. As it was said before, the storage of all data is not convenient and not possible, however there does not exist a precise method of defining the parameters m and x_0. Therefore we shall make a compromise: we shall assess the parameters by the method of moments.

Let us presume that the first two moments of the sample are known

$$m_1 = \frac{1}{r}\sum_{i=1}^{r} t_i , \quad m_2 = \frac{1}{r}\sum_{i=1}^{r} t_i^2 . \tag{39}$$

Precise meanings of the prior moments of the Weibull distribution [2]:

$$m_1 = x_0^{1/m}\Gamma\left(1+\frac{1}{m}\right), \quad m_2 = x_0^{2/m}\left(1+\frac{2}{m}\right). \tag{40}$$

Having equalised the meanings of sample parameters to their analytical expressions, we shall obtain the system of equations enabling to find x_0 and m: $x_0^{1/m}\Gamma\left(1+\frac{1}{m}\right) = m_1$, $x_0^{m/2}\Gamma\left(1+\frac{2}{m}\right) = m_2$.

After rearrangement of the system of non-linear equations, i.e. after division of the second one from the first square is $\dfrac{x_0^{2/m}\Gamma\left(1+\frac{2}{m}\right)}{x_0^{2/m}\Gamma\left(1+\frac{1}{m}\right)\Gamma\left(1+\frac{1}{m}\right)} = \dfrac{\hat{m}_2}{\hat{m}_1}$.

Since $\Gamma(a+1) = \Gamma(a)a$, then

$$\frac{\Gamma\left(\frac{2}{m}\right)\frac{2}{m}}{\Gamma\left(\frac{1}{m}\right)\Gamma\left(\frac{1}{m}\right)\frac{1}{m^2}} = \frac{2m\Gamma\left(\frac{2}{m}\right)}{\Gamma\left(\frac{1}{m}\right)\Gamma\left(\frac{1}{m}\right)} = \frac{\hat{m}_2}{\hat{m}_1^2} . \tag{41}$$

By the application of the Lagrange's formula for the gamma function argument of equation [2] is $\Gamma(2z) = 2^{2z-1}\pi^{-1/2}\Gamma(z)\Gamma\left(z+\frac{1}{2}\right)$. From (41) we obtain much more convenient phenomenon for obtaining the m:

$$\hat{m}_1^2 2^{2/m} m\Gamma\left(\frac{1}{m}+\frac{1}{2}\right) - \hat{m}_2^1\sqrt{\pi}\Gamma\left(\frac{1}{m}\right) = 0 . \tag{42}$$

The quantity m is obtained by solving the equation (42), and x_0 – by the obtained meaning and by one of (40) equations, for example

$$x_0 = \left[\frac{m_1}{\Gamma\left(1+\frac{1}{m}\right)}\right]^m . \tag{43}$$

Searching for the parameters x_0 and m by (42), (43) and (39), stored are only the statistics

$$\hat{m}_t = \left(\frac{1}{w}\right)\sum t_i , \quad \hat{m}_2 = \left(\frac{1}{w}\right)\sum t_i^2 .$$

The method of moments gives non-optimal assessment of the meanings m and x_0. The quantities of small samples m and x_0, are calculated by the method of moments and they may differ from the calculated ones by the method of maximum simplicity, therefore, given a small n it is purposeful to calculate m and x_0 by the latter method and thereto it is necessary to remember all the meanings $t_1, ..., t_r$. For a large n it is better to use the method of moments.

Finally, it should be mentioned that stochastic models have to reflect the main regularities of the investigated object. The degree of adequacy in the given case depends on how precisely in the models is assessed the interdependency between incoming and outgoing parameters, interactive system and environment, ability to correct by a model the decisions and finally – the application of stochastic methods in obtaining the optimal behaviour scheme of the investigated system.

Conclusions

- ☆ Generally the technical-economic indices of transportation should be analysed as random factors, which are random to each meaning of the argument as well. Arguments mean the time and other parameters of the technological transportation process. Thus the optimum criteria should be considered not as determined but as random ones.
- ☆ Most indices according to which the technological transportation process is assessed, are interconnected, therefore it should be taken into account that these indices are used as criteria of optimality. For the determination of digital characteristics of the technical-economical indices according to the statistical information received during the technological transportation process, the mathematical probability assessment as well as correlation and dispersion functions should be calculated.
- ☆ For the modelling of transport networks and the flows of freight and transport means in them, it is purposeful to describe analytically the random factors by the non-parametric assessment. Differently from parametric, the non-parametric assessment of distribution density has a number of merits. Firstly, when in the course of time the distribution density type of flows is changing, it is possible to approximate with precision sufficient for practical use. Secondly, this assessment is significantly less sensitive to data errors.
- ☆ Statistical information on freight and transport flows is renewed and replenished in the course of time. The costs of its storage increase too with the growth of information amount. Therefore it is necessary to obtain the required statistical assessment with the least information amount. The mathematical models necessary for accumulation of statistics are created and verified on this purpose. There have been created models for the following cases, when the density of distribution of random factors is assessed by: a) the Bayesian analysis; b) the normal distribution; c) the logarithmic-normal; d) the non-parametric distribution; e) the Weibull distribution. There are created the algorithms for accumulation of minimum statistical data to all these cases.

References

[1] Candle L. M., Stewart A. (1966) *The theory of distribution.* Nauka, Moscow. 584p. *(in Russian)*
[2] Winkler R. L. (1967) The Assessment of prier Distribution in Bayesian Analysis. J. Amer. Stat. Ass. **62**, No 319, 320 –382
[3] Baytman P., Erdain A. (1965) *The higher transcendental functions.* Nauka, Moscow. 343p. *(in Russian)*
[4] Baublys A. (2002) Statistical models for vehicle fleet management, *Transport and Telecommunication,* **3**, No 3, 4–22

Received on the 15th of March 2004

Computer Modelling & New Technologies, 2004, Volume 8, No.1, 39-47
Transport and Telecommunication Institute, Lomonosov Str.1, Riga, LV-1019, Latvia

A FAST AND ROBUST WATERMARKING METHOD FOR JPEG IMAGES

W. LUO[1], G.L. HEILEMAN[2]

[1]Engineering Department, St. Mary's University, San Antonio, TX 78228, U.S.A.
E-mail: wluo@stmarytx.edu
[2]Department of Electrical and Computer Engineering, University of New Mexico, Albuquerque, NM 87131, U.S.A.

In this paper, a JPEG domain image watermarking method that utilizes spatial masking is presented. The watermarking algorithm works in the compressed domain, and can be implemented efficiently in real-time (only 50ms is required for a 512x512 24-bit color image on a 700MHz computer). In many applications, particularly those associated with delivering images over the Internet, the ability to watermark images in real-time is required. In order to achieve a real-time watermarking capability, the proposed technique avoids many of the computation steps associated with JPEG compression. Specifically, the forward and inverse DCT do not need to be calculated, nor do any of the computations associated with quantization. Robustness to JPEG compression, different kinds of noise (additive, salt & pepper, and speckle) and image cropping attacks are achieved with the proposed system, and the relationship between watermark robustness and watermark position is described. A further advantage of the proposed method is that it allows a watermark to be detected in an image without referencing to the original unwatermarked image, or to any other information used in the watermark embedding process.
Keywords: *image watermarking, spatial masking*

1. Introduction

The success of the Internet, cost-effective and popular digital recording and storage devices, and the promise of higher bandwidth and quality of service (QoS) for both wired and wireless networks has made it possible to create, replicate, transmit, and distribute digital content in an effortless way [1,7]. The need for developing watermarking techniques that protect electronic information has become increasingly important due to the widespread availability of methods for disseminating exact copies of this information (e.g., via the Internet), and the ease with which this information can be reproduced [2,6,8]. Digital watermarking is increasingly being used for the purposes of protecting digital content against unauthorized usage or theft, and for documenting or ensuring (i.e., verifying, guaranteeing, or proving) the integrity of multimedia content. Digital image watermarking involves the embedding of additional information into an image in a manner that is imperceptible to the human observer, but which can be discovered by watermark detection algorithms. Digital image watermarking is typically performed in either the frequency or spatial domain. Early digital image watermarking methods used the spatial domain to perform watermark embedding by simply changing the least significant bit of each pixel in order to encode a message. It has been found that transform domain watermarking schemes are typically much more robust to image manipulation as compared to spatial domain schemes. The method proposed here belongs to frequency domain watermarking category, and in particular involves modifications to the discrete cosine transform (DCT) domain coefficients.

In the DCT domain, watermarks should be embedded in those coefficients that meet the following requirements in order for the watermarks to be invisible and also robust against attacks aimed at removing them [3]. First, watermark embedding should target those coefficients having large perceptual capacity, allowing strong watermarks (strong against attacks) to be embedded without perceptual distortion. Second, the embedding should focus on those coefficients that will change little when common image processing and noise corruption attacks are applied. This should include both intentional and unintentional attack possibilities.

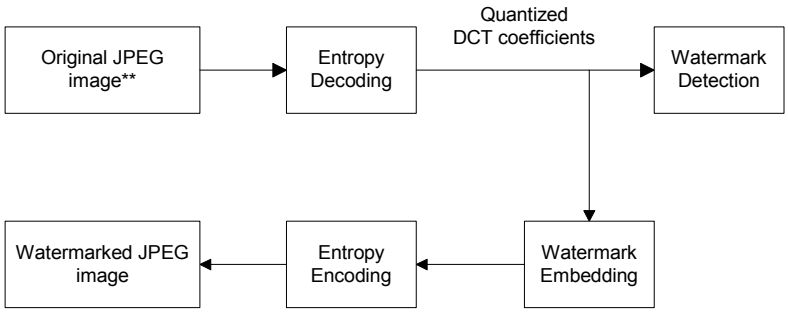

Figure 1. The proposed watermarking system

In many applications related to Internet-based delivery of images, particularly those associated with large image databases; there are requirements for real-time watermark insertion and extraction. The method described in this paper was developed with these requirements in mind. In particular, this method is capable of embedding a watermark in a 512x512 24-bit color JPEG image in approximately 50ms using a 700MHz computer. Watermark detection and extraction are similarly fast, and do not require access to the original (unwatermarked) image, or to any other information used in the watermark embedding process, in order to detect and extract the watermark. Thus, costly searches through an image database can be avoided during the watermark detection/extraction process.

2. Watermarking Method

JPEG compression method starts by dividing an image into disjoint 8x8 blocks of pixels. Next, for each block, the forward DCT is calculated, producing 64 DCT coefficients. Let us denote the (x, y)-th DCT coefficient of the k-th block as $d_k(x,y)$, $0 \le x, y \le 7$, $k = 1, \cdots, B$, where B is the total number of blocks in the image. In each block, all 64 coefficients are further quantized to integers $D_k(x,y)$ using a JPEG quantization matrix Q:

$$D_k(x,y) = R\left(\frac{d_k(x,y)}{Q(x,y)}\right), \tag{1}$$

where R denotes the integer round operation. The quantized coefficients are then arranged in a *zig-zag* manner denoted by $Z_k(i)$, $0 \le i \le 63, k = 1, \cdots, B$, and compressed using a Huffman coder. The resulting compressed stream, together with a header, forms the JPEG compressed image file. For robustness and simplicity reasons, the method described here embeds watermarks in the luminance (Y) component of an image, leaving the chromatic components (C_b and C_r) intact. The general model for the watermarking system is shown in Figure 1. Note that for the watermark detection/extraction process, we assume that the input to the system (i.e., the "original JPEG image") is the watermarked, and possibly attacked, image.

The specific computations performed at each step in the watermarking embedding process are as follows:

- Read the original JPEG image, and for each block k, perform entropy decoding in order to obtain the quantized DCT coefficients $Z_k(i)$, $0 \le i \le 63, k = 1, \cdots, B$
- Let i_0 denote the initial coefficient within the coefficient block (in *zig-zag* order) where watermark insertion begins. Then, in four adjacent DCT coefficient blocks, as shown in Figure 2, a single bit w is embedded as follows:

8x8 DCT block 1	8x8 DCT block 2
8x8 DCT block 3	8x8 DCT block 4

Figure 2. An embedding unit

if $w = 1$ **then**
if $Z_1(i_0) < \overline{M} + \delta$ **then** $Z_1^*(i_0) = \overline{M} + \delta$
else ($w = 0$)
if $Z_1(i_0) < \overline{M} - \delta$ **then** $Z_1^*(i_0) = \overline{M} - \delta$

where $\overline{M} = R((Z_2(i_0) + Z_3(i_0) + Z_4(i_0))/3)$, and δ is determined by the local characteristics of the image. Specifically, let $M_{\max}$ = max $\{ Z_1(i_0),\ Z_2(i_0),\ Z_3(i_0),\ Z_4(i_0) \}$, $M_{\min}$ = min $\{ Z_1(i_0),\ Z_2(i_0),\ Z_3(i_0),\ Z_4(i_0) \}$, and assume T_1 and T_2 are two adjustable threshold values with $T_1 < T_2$. Then, δ is computed as follows:

$\delta = 1$, if $(M_{\max} - M_{\min}) \le T_1$; $\delta = 2$, if $T_1 < (M_{\max} - M_{\min}) \le T_2$; $\delta = 3$, if $T_2 < (M_{\max} - M_{\min})$.

The algorithm uses the fact that the relationship between DCT coefficients at the same position in different 8x8 blocks of an image will hold even if these coefficients are quantized by an arbitrary quantization table in the JPEG compression process [5]. The algorithm also exploits the fact that $Z_1(i_0)$ is usually close to $\overline{M}$.
Since the visibility of the superimposed watermark signal is affected by the background texture [3], the stronger the texture in the background, the lower the visibility of the embedded signal will be (this is texture masking) [4]. The method therefore embeds a stronger watermark signal in stronger texture areas.

- Replace $Z_1(i_0)$ with the new coefficients $Z_1^*(i_0)$. The above procedure is applied to all four DCT coefficient adjacent blocks. The final watermarked image I^* is then obtained by entropy encoding these modified DCT blocks.

Watermark extraction is the inverse of the watermark embedding procedure. Suppose that I^* is the signal-distorted or maliciously-attacked watermarked image. To extract the watermark from I^*, $\overline{M}^*$ is calculated from $Z^*(i_0)$ in the same way as in step 2 above. Then, the watermark w is extracted according to following rule:

if $Z_1^*(i_0) > \overline{M}^*$ **then** $w = 1$ **else** ($Z_1^*(i_0) \le \overline{M}^*$) $w = 0$.

The experiments detailed in the section 4 were used to quantify the performance of this watermarking system.

3. Watermark Mixing

Visually meaningful pattern, such as letters and logos, can serve as a quick check for ownership. Shown in Figure 3 is a 53x53 binary pattern “EECE”.

Figure 3. Original watermark

The decision on whether an image is watermarked or not can be made by (automatically) comparing the extracted pattern with the original one, if available, or by human (e.g., jury in court) based on visualizing the extracted pattern. The latter case uses a reasonable assumption that human can distinguish a “meaningful” pattern from a random one. It is also possible to make such decision automatically, e.g., computing a randomness measure. Obviously, without appropriate adjustment for the spatial relationship of the watermark, a common image cropping operation may destroy the visual pattern of embedded watermark.

To survive image cropping, a two-dimensional “torus automorphism” is used to permute (or mix) the watermark to disperse its spatial relationship. A two-dimensional “torus automorphism” can be considered like a spatial transformation of planar regions which belong in a square two-dimensional area. The set of torus automorphisms is special subset of Anosov diffeomorphisms, which exhibit strongly chaotic motion i.e. local instability, ergodicity, mixing and decay of correlations [9]. A great subset of torus automorphisms is represented by the family of one-parameter systems which is defined as follows:

$$A_N(k): L \to L \quad \begin{pmatrix} x_{n+1} \\ y_{n+1} \end{pmatrix} = \begin{pmatrix} 1 & 1 \\ k & k+1 \end{pmatrix} \begin{pmatrix} x_n \\ y_n \end{pmatrix} (\mathrm{mod}\, N) \tag{2}$$

where $(x_n, y_n) \in L = [0, N-1] \times [0, N-1]$. For the $N-1$ integer values of k in the domain $[1, N)$ we obtain a finite family of systems $A_N(k)$. For any integer lattice L of size N there is an integer $P = P(k, N)$ such that

$$A_N^P(k)\xi = \xi \ (\mathrm{mod}\, N), \quad \forall \xi \in L. \tag{3}$$

We call the integer P "recurrence time". Thus any lattice point is a fixed point under the action of $A_N^P(k)$ and also the periodicity condition $A_N^{i+jP}(k)\xi = A_N^i(k)\xi$ holds, for all positive integers i, j and for all $\xi \in L$.

In Figure 4, the watermark is mixed using torus automorphism $A_{53}^5(1)$ to survive image cropping.

Figure 4. Mixing of binary pattern "EECE" by $A_{53}^5(1)$

4. Experimental Results

The similarity measurement ``Normalized Correlation" (*NC*) between the original watermark w and the extracted watermark $\overline{w}$ is defined as:

$$NC = \frac{\sum_i \sum_j w(i,j)\overline{w}(i,j)}{\sum_i \sum_j [w(i,j)]^2}.$$

This provides objective judgment of the extracting fidelity.

The experiments described here compare the performance of different embedding strategies in terms of robustness against JPEG compression, different kinds of noise, and image cropping attacks. The two standard color images shown in Figure 5, *lenna* and *baboon*, were used in our experiments. All watermarked images derived from these test images were 512x512 pixels and 24-bits in color.

First the two test images were JPEG compressed by quality factor 75. Next, the same watermark was embedded into these two compressed images using parameters $T_1 = 15$, $T_2 = 30$, and at various coefficient locations determined by i_0, $0 \le i_0 \le 63$. The average watermarking time of the proposed system was approximately 50ms using a 700MHz computer. A single bit was embedded in a 2x2 block, and in total 1024 bits were embedding in an image. Figure 5 shows the original and the watermarked images, respectively, when $i_0 = 10$. The method does not cause perceptible changes to be introduced into the watermarked images.

The first experiment studies the effects of watermark embedding at various positions ($i_0 = 0, 2, 4, 6, 8, 10$, and 12) on the peak signal-to-noise ratio (PSNR), which is calculated as the difference between the original test image and the watermarked image.

From Figure 6, we see that images containing stronger texture features, e.g., *baboon* will yield a lower PSNR. This is exactly what we want to achieve with texture-based watermarking. That is, the goal is to always embed stronger watermark signals into rich texture areas.

The next set of experiments details watermark robustness to JPEG compression. The watermarked images, embedded with parameters $i_0 = 0, 2, 6$, and 10, were attacked by JPEG compression at different quality levels. The results are shown in Figures 7 (a), (b), and (c). From Figures 7 (a) and (b), it is obvious that watermarks embedded at lower frequencies are more robust than watermarks embedded at higher frequencies. Also, Figure 7 (c), with $i_0 = 10$, shows that the watermark

in *baboon* is more robust to JPEG compression attacks than the one in *lenna*. This is because the watermark in *baboon*, as described above, is embedded stronger due to the spatial masking used during watermark embedding. Another experiment studies watermark robustness to additive noise attacks. The watermarked images ($i_0 = 10$) are attacked by additive Gaussian noise at different energy levels. The results are presented in Figure 7 (d). It is easy to see from this figure that the watermarked images are very robust to additive noise attacks.

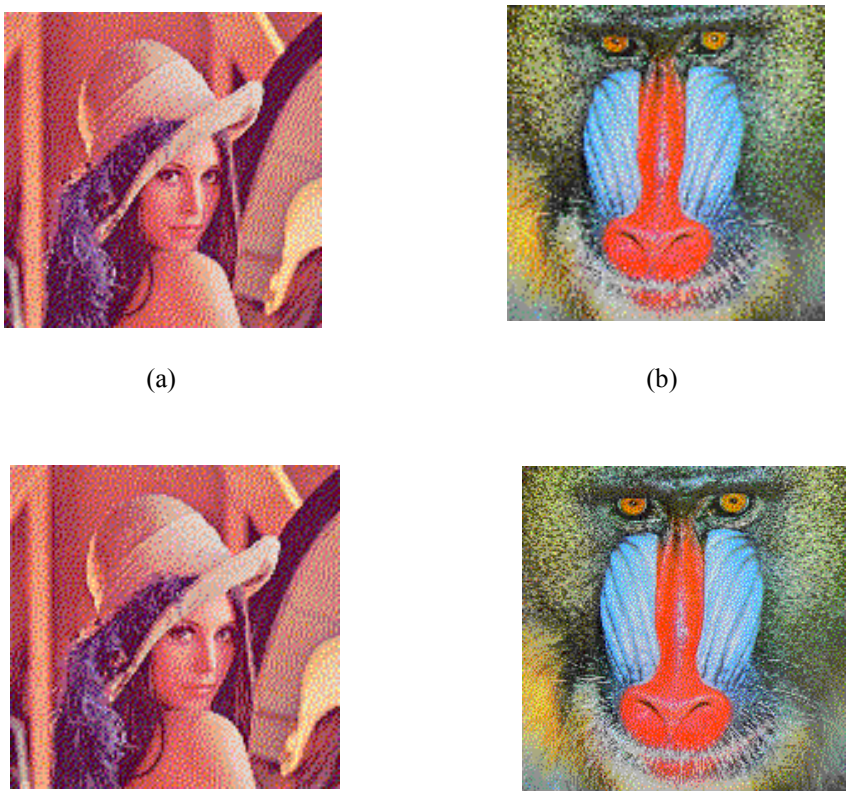

(a) (b)

(c) (d)

Figure 5. The original images (a) *lenna* and (b) *baboon* and the corresponding watermarked versions (c) and (d)

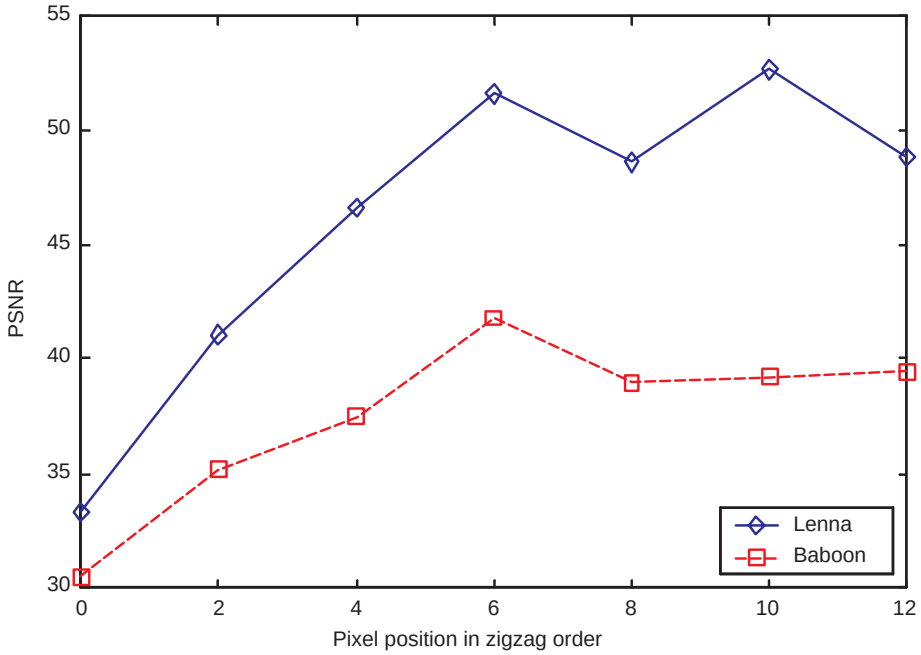

Figure 6. The effects of watermark embedding on PSNR

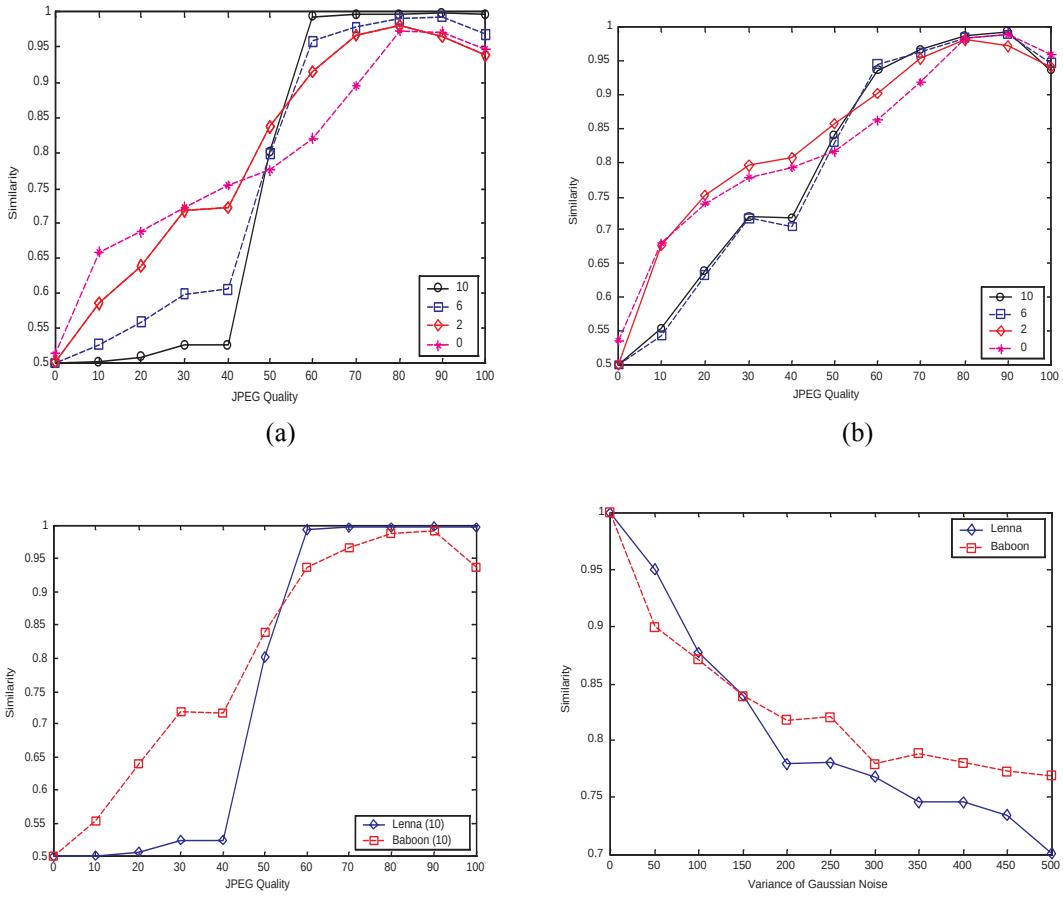

Figure 7. Comparison of watermark robustness to JPEG compression relative to watermark position in (a) *lenna* and (b) *baboon*; (c) comparison of watermark robustness to JPEG compression relative to specific images (with different texture components); (d) comparison of watermark robustness to additive noise attack for the watermarked *lenna* and *baboon* images

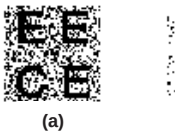

Figure 8. Recovered watermark from *lenna* after JPEG compression attack

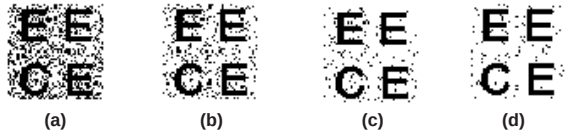

Figure 9. Recovered watermark from *baboon* after JPEG compression attack

TABLE 1. *NC*s of recovered watermarks after JPEG attack

Figure	**(a)**	**(b)**	**(c)**	**(d)**
Q	50	60	70	80
NC (lenna)	0.65	0.91	0.97	0.97
NC (baboon)	0.69	0.85	0.93	0.96

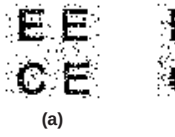

Figure 10. Recovered watermark from *lenna* after Gaussian additive noise attack

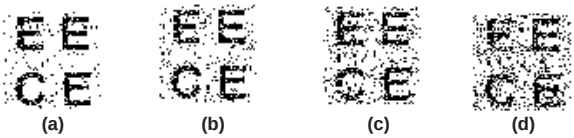

Figure 11. Recovered watermark from *baboon* after Gaussian additive noise attack

TABLE 2. *NC*s of recovered watermarks after Gaussian additive noise attack

Figure	**(a)**	**(b)**	**(c)**	**(d)**
Variance	20	50	100	200
NC (lenna)	0.95	0.88	0.81	0.77
NC (baboon)	0.95	0.91	0.87	0.81

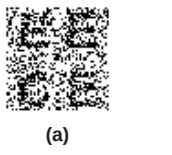

Figure 12. Recovered watermark from *lenna* after salt & pepper noise attack

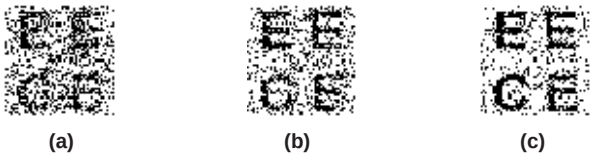

Figure 13. Recovered watermark from *lenna* after speckle noise attack

Figure 14. Recovered watermark from *lenna* after image cropping attack

TABLE 3. *NC*s of recovered watermarks after salt & pepper noise attack

Figure	**(a)**	**(b)**	**(c)**
Density	0.02	0.01	0.005
NC	0.72	0.81	0.86

TABLE 4. *NC*s of recovered watermarks after speckle noise attack

Figure	**(a)**	**(b)**	**(c)**
Variance	0.02	0.01	0.005
NC	0.72	0.79	0.85

TABLE 5. *NC*s of recovered watermarks after image cropping attack

Figure	**(a)**	**(b)**	**(c)**
Cropping ratio	25%	50%	Random cropping
NC	0.72	0.50	0.80

Finally, we conducted a series of experiments by embedding the visual pattern in Figure 4 into the original image to further test the watermarking effects and robustness of our watermarking scheme to JPEG compression, different kinds of noise (Gaussian, salt & pepper, and speckle), and image cropping attacks when it is used in some real applications.

- First, different JPEG compression qualities ($Q = 50, 60, 70, 80$) are applied to the watermarked image. The recovered visual patterns after JPEG attack are shown in Figures 8 and 9. The *NC*s of recovered watermarks and the corresponding JPEG compression qualities Q are listed in Table 1.
- Second, different kinds of noises with different variances and densities are applied to the watermarked image. The recovered visual patterns after different noise attacks are shown in Figures 10-13. The *NC*s of recovered watermarks and the corresponding variances and densities are listed in Tables 2-4.
- The last experiment studies watermark robustness to image cropping attacks. We cropped the watermarked image with different cropping ratios (25%, 50% and random cropping). The recovered visual patterns after image cropping attacks are shown in Figure 14. The *NC*s of recovered watermarks and the corresponding cropping ratios are listed in Table 5.

From the experiments above, we see that the embedded visual watermark was shown to be robust to JPEG compression, different kinds of noise and image cropping attacks.

5. Conclusions

In this paper, we have proposed a fast and robust JPEG domain image watermarking method. The proposed method can be implemented very efficiently, requiring approximately 50ms to embed or extract a watermark using a 700MHz computer. The embedded watermark was experimentally shown to be robust to JPEG compression, different kinds of noise (additive, salt & pepper, and speckle) and image cropping attacks, and can be extracted without reference to the original (unwatermarked) image and embedding parameters. Also, the experiments described here show that embedding watermarks in coefficients, which are "important" for the image, are more likely to retain embedded watermark data, despite attacks that result in visually unimportant distortions. Correct choices for the threshold values T_1 and T_2 are of fundamental importance for watermark invisibility and good detector/extractor performance. It is possible to adjust the threshold values according to different image features, and even add additional threshold level. So, our watermarking scheme is very flexible, and can be tailored to meet the requirements of different real applications.

6. Acknowledgements

The authors are grateful to Elisar Software Corporation for providing financial support for this research.

References

[1] Cox I.J., Bauml R., and Girod B. Digital Watermarking, *Academic Press*, 2002.
[2] Hartung F., and Kutter M. Multimedia Watermarking Techniques, *Proc. IEEE*, Vol. 87, No. 7, pp. 1079-1107, 1999.
[3] Huang J. and Shi Y.Q. and Shi Y. Embedding Image Watermarks in DC Components, *IEEE Trans. on circuits and systems for video technology*, Vol. 10, pp. 974-979, 2000.
[4] Langelaar G.C. and Lagendijk R.L. Optimal Differential Energy Watermarking of DCT Encoded Images and Video, *IEEE Trans. on image processing*, Vol. 10, pp. 148-158, 2001.
[5] Lin C.Y. and Chang S.F. A Robust Image Authentication Method Distinguishing JPEG Compression from Malicious Manipulation, *IEEE Trans. on circuits and systems for video technology*, Vol. 11, pp. 153-168, 2001.
[6] Petitcolas F.A.P., Anderson R.J., and Kuhn M.G. Information Hiding - A Survey, *Proc. IEEE*, Vol. 87, No. 7, pp. 1062-1078, 1999.
[7] Podilchuk C.I. and Delp E.J. Digital Watermarking Algorithms and Applications, *IEEE Signal Processing Magazine*, Vol. 7, pp. 33-46, 2001.
[8] Swanson M.D., Kobyashi M., and Tewfik A.H. Multimedia Data-Embedding and Watermarking Technologies, *Proc. IEEE*, Vol. 86, No. 6, pp. 1064-1087, 1998.
[9] Voyatzis G. and Pitas I. Applications of Toral Automorphisms in Image Watermarking, *Proc. of ICIP96*, Vol. 2, pp. 237-240, 1996.

Received on the 20th of April 2004

Computer Modelling & New Technologies, 2004, Volume 8, No.1, 48-52
Transport and Telecommunication Institute, Lomonosov Str.1, Riga, LV-1019, Latvia

ОСОБЕННОСТИ РАСЧЁТА АВИАЦИОННЫХ ИНДУКТОРНЫХ ГЕНЕРАТОРОВ

А. Д. СЕРЕБРЯКОВ

Институт транспорта и связи
Ломоносова, 1, LV – 1019, Рига, Латвия

Получено аналитическое выражение для определения воздушного зазора аксиального индукторного генератора. Рассмотрена методика учёта реакции якоря.

Analytical expression for definition of the air-gap of the axial inductor generator is obtained. The procedure of the account of reaction of an anchor is considered.
Keywords: *inductor generator, anchor reaction, air-gap*

Индукторные электрические машины (ИЭМ) нашли достаточно широкое применение в железнодорожном и автомобильном транспорте в качестве генераторов, а также в различных отраслях техники в виде электромашинных преобразователей для сварки, индукционного нагрева и других целей.

В авиации впервые индукторные генераторы мощностью 2 кВт и частотой 1000 Гц, разработанные В. П. Вологдиным в 1912 г., были применены для питания радиостанции на самолёте «Илья Муромец». В дальнейшем они нашли применение в качестве однопакетных аксиальных генераторов в электромашинных преобразователях типа МА мощностью от 100 до 1500 В · А (МА – 100; 250; 500; 1500).

Для авиации наиболее перспективными качествами ИЭМ являются их конструктивная простота и высокая надёжность, а сдерживающим фактором – большее, чем в обычных синхронных машинах, значение удельной массы.

Однако, во-первых, в настоящее время традиционный критерий уровня бортового оборудования – его масса – отступает на второй план, поскольку его сокращение уже не даёт существенного экономического эффекта. На первый план выступают необходимость повышения общей безопасности полётов и сокращение эксплутационных расходов.

Таким образом, вес агрегата не является доминирующим фактором, определяющим возможность применения агрегата в авиации; основным фактором выступает его надёжность.

Во-вторых, работа над совершенствованием ИЭМ позволила уменьшить удельную массу и приблизить её к значениям применяемых электрических машин / 1 /.

Эти обстоятельства позволяют говорить о возможности применения ИЭМ в авиации в качестве генераторов, различных двигателей, сельсинов и т.д. / 2 / и на этой основе повышать эффективность эксплуатации и технического обслуживания бортового оборудования.

Индукторная машина имеет зубчатую структуру пакетов статора и ротора – чередование зубцов и впадин (пазов), что и определяет изменение магнитной проводимости воздушного зазора между ними, пульсацию магнитного потока и наведение ЭДС в обмотке якоря. Такая компоновка определяет некоторые особенности реакции якоря в ИЭМ по сравнению с обычной явнополюсной синхронной машиной и соответствующие особенности учёта реакции якоря при расчёте машин и, в частности, при определении воздушного зазора.

В системе электроснабжения воздушных судов генераторы переменного тока работают при активно – индуктивной нагрузке ($\cos(\varphi_н) = 0.8 \ldots 0.85$). В этом случае имеет место как продольная, так и поперечная реакция якоря. Продольная реакция якоря вызывает значительное уменьшение индукции под зубцом и увеличение индукции под пазом ротора. Поперечная реакция якоря вызывает значительное искажение формы кривой поля / 3 /. Это обусловливает изменение гармонического состава магнитного потока в зубцах, изменение соотношения между постоянными и гармоническими составляющими магнитных потоков, а также проявляется в изменении и смещении их максимумов от начала отсчёта углов поворота ротора.

Результирующее магнитное поле на участке зубцового шага ротора t_{ZR} распределяется неравномерно и имеет резко выраженный пик между продольной d и поперечной q осями машины

(см. / 3 /, стр. 134, рис. 4.13, в). Амплитуда пика превышает в три и более раз амплитуду первой гармонической составляющей магнитной индукции. Это может вызывать дополнительное насыщение магнитной цепи. Поэтому кроме обычного учёта реакции якоря, осуществляемого в явнополюсных синхронных машинах путём включения в МДС возбуждения эквивалентных значений МДС реакции якоря, необходимо в ИЭМ выполнять ещё проверку на возможность насыщения зубцов статора и ротора из-за влияния реакции якоря.

Приведенные к обмотке возбуждения составляющие МДС реакции якоря F_{ad} и F_{aq} определяются следующим образом:

$$F_{ad} = K_d \cdot F_{d1};\ F_{aq} = K_q \cdot F_{q1}, \quad (1)$$

где K_d, K_q – коэффициенты приведения, причём для индукторной машины они рассчитываются через проводимости воздушного зазора; F_{d1}; F_{q1} – первые гармонические МДС реакции якоря по осям d и q, которые могут быть определены как

$$F_{d1} = F_{a1} \cdot \sin(\Psi);\ F_{q1} = F_{a1} \cdot \cos(\Psi). \quad (2)$$

Здесь Ψ – угол сдвига по фазе между ЭДС холостого хода E_0 и током якоря I; F_{a1} –МДС обмотки якоря по первой гармонической, которая для трёхфазных одноимённо- или разноимённополюсных генераторов может быть определена в соответствии с выражением

$$F_{a1} = 1.35 \cdot I_1 \cdot W_ф \cdot \frac{K_\omega}{Z_r}, \quad (3)$$

где $W_ф$ – число витков в фазе обмотки якоря; K_ω – обмоточный коэффициент по первой гармонической; Z_r – число зубцов ротора; I_1 – действующее значение тока якоря первой гармоники.

Значение sin (Ψ) может быть определенно как

$$\sin(\Psi) = \frac{X_c}{\sqrt{(R_a + R_{нг})^2 + X_c^2}}, \quad (4)$$

где R_a, X_c – активное и синхронное сопротивления обмотки якоря; $R_{нг}$ – сопротивление нагрузки.

Учёт размагничивающего действия реакции якоря может быть также осуществлён с помощью коэффициента увеличения потока и ЭДС при нагрузке

$$K_E = \frac{\sqrt{(R_a + R_{нг})^2 + X_c^2}}{R_a + R_{нг}} \text{ или } K_E = \frac{\sqrt{U_{фр}^2 + (I_1 \cdot X_c)^2}}{U_{фр}} \quad (5)$$

где $U_{фр}$ – расчётное фазное напряжение обмотки якоря.

В этом случае необходимая МДС возбуждения

$$F_B = n_\delta \cdot K_E \cdot F_{\delta э}, \quad (6)$$

где n_δ – число последовательно включенных воздушных зазоров на пути потока возбуждения; $F_{\delta э}$ – МДС эквивалентного воздушного зазора $\delta_э$.

Значением δэ обычно задаются в начале расчёта, принимая его ориентировочно равным $\delta_э = (1.2 \ldots 1.5) \cdot \delta$, причём δ – реальный воздушный зазор, его увеличением до $\delta_э$ учитывается МДС стали.

Значение $\delta_э$ учитывается и при расчёте магнитных проводимостей полюсных выступов статора: удельная проводимость зазора $\lambda_\delta = \frac{b_{zs}}{\delta_э}$, а при определении проводимостей пазов используется отношение $\frac{b_{пs}}{\delta_э}$ (b_{zs}, b_{ns} – ширина зубца и паза статора).

Затем в ходе расчёта магнитной цепи величина $\delta_э$ подвергается проверке, при которой:
а) определяется удельная МДС воздушного зазора (то есть МДС на 1 мм воздушного зазора)

$$F_{\delta 1} = \frac{B_\delta \cdot \delta_1}{\mu_0}, \quad (7)$$

причём B_δ – индукция в воздушном зазоре, Тл; $\delta_1 = 1 \cdot 10^{-3}$ м – воздушный зазор в 1 мм; $\mu_0 = 4 \cdot \pi \cdot 10^{-7}$ Гн/м – магнитная постоянная;
б) затем оценивается значение дополнительного расчётного зазора $\Delta\delta = \delta_э - \delta$ по выражению

$$\Delta\delta = \frac{F_z}{F_{\delta 1}}, \tag{8}$$

где F_z – МДС зубцов статора и ротора, который и сравнивается с принятым;
в) реальный воздушный зазор

$$\delta = \frac{\delta_э \cdot (F_{\delta э} - F_z)}{F_{\delta э}}, \tag{9}$$

где $F_{\delta э} = \frac{B_\delta \cdot \delta_э}{\mu_0}$. (10)

При выборе значения магнитной индукции B_δ для ИЭМ исходят обычно из допустимого значения индукции в зубцах якоря B_{zs}. Это связано с тем, что насыщение зубцов якоря уменьшает модуляцию магнитного потока, а следовательно, его использование. Величина B_{zs} с повышением частоты снижается из-за вытеснения потока в стали и высоких удельных потерь.

Значения B_δ и B_{zs} связаны соотношением

$$B_{zs} = \frac{(1.05\ldots1.1) \cdot B_\delta \cdot b_{zr}}{b_{zs} \cdot K_{cт}}, \tag{11}$$

где b_{zr}, b_{zs} – ширина зубцов ротора и статора; $К_{ст}$ – коэффициент заполнения пакетов сталью.

Для выбора машины с меньшей степенью влияния реакции якоря целесообразно:
а) вначале увеличить индукцию в воздушном зазоре при холостом ходе $B_{\delta 0}$, что при заданной ЭДС обусловит уменьшение числа витков обмотки якоря, и следовательно, её индуктивное сопротивление; после определения коэффициента $К_E$ (5) индукция в зазоре при нагрузке будет примерно равна

$$B_{zs} = \frac{B_\delta}{K_{cт} \cdot K_E}; \tag{12}$$

б) во втором случае, выбрав вначале значение $B_\delta < B_{\delta 0}$ и произведя расчёт магнитной цепи, определяем коэффициент $К_E$ (5) и затем индукцию в зубцах статора

$$B_{zs} = \frac{B_\delta \cdot K_E}{K_{cт}}. \tag{13}$$

Сравнивая оба результата, выбираем тот, который обеспечивает меньшее значение индукции в зубце при нагрузке, то есть меньшее насыщение зубцов, являющихся «узким» местом в магнитной цепи ИЭМ.

Влияние насыщения магнитной цепи ИЭМ может быть учтено соответствующим расчётом значений коэффициентов постоянной и гармонических составляющих магнитной проводимости полюсных выступов / 1 /.

Независимо от выбранной методики учёта реакции якоря и насыщения зубцов необходимо осуществлять проверку по предельно-допустимому влиянию реакции якоря на насыщение магнитной цепи ИЭМ. Критерием допустимости этого влияния служит коэффициент $К_a$, равный отношению максимальной МДС обмотки якоря $F_{a.max}$ к МДС возбуждения $F_{B\delta}$, необходимой для проведения магнитного потока через воздушные зазоры (то есть без учёта влияния МДС якоря):

$$K_{\text{а}} = \frac{F_{\text{a.max}}}{F_{\text{В}\delta}}. \tag{14}$$

Значения $F_{a.max}$ и $F_{в\delta}$ могут быть определены как

$$F_{\text{a.max}} = \sqrt{m} \cdot \sqrt{2} \cdot I_{\text{ан}} \cdot W_{\text{ка}}; \tag{15}$$

$$F_{в\delta} = K_{в} \cdot n_{\delta} \cdot F_{\delta} = \frac{K_B \cdot n_{\delta} \cdot B_{\delta} \cdot \delta}{\mu_0}, \qquad (16)$$

где $I_{ан}$ – номинальный ток в обмотке якоря; $W_{ка}$ – число витков катушки обмотки;
$K_{в} = (1.2 \ldots 1.4)$ – коэффициент учёта МДС стали.

Значения K_a должно находиться в пределах (0.5 … 0.55) для обычных электротехнических сталей (например, ст. 2211 – 2411) и быть в пределах (0.6 …0.65) для сталей с повышенной индукцией насыщения (например, ст. 49К2Ф, имеющая $B_{н} = 2.2$ Тл).

Величина рабочего воздушного зазора δ во многом определяет эффективность работы ИЭМ. По технологическим условиям желательно выбирать воздушный зазор бóльшим. Но при увеличении δ уменьшается переменная составляющая магнитного потока, ЭДС обмотки якоря и мощность ИЭМ.

Рекомендуемые выражения для предварительного выбора δ в виде

$$\delta \geq 0.02 + \frac{\sqrt{D \cdot l}}{500} \text{ (см) и } \delta = \left(\frac{1}{200} \ldots \frac{1}{300}\right) \cdot D \qquad (17)$$

определяют диапазон возможных значений δ и не дают однозначного ответа. В (17) D, l – диаметр расточки и длина пакета якоря соответственно.

По техническим и технологическим характеристикам наибольшую вероятность для применения в авиации имеют одноименнополюсные двухпакетные аксиальные индукторные генераторы (/ 3 /, стр.161, рис. 6.2).

Применительно к подобным конструкциям значения числа витков в катушке обмотки якоря $W_{ка}$ и индуктивного сопротивления фазы обмотки якоря X_a могут быть определены как

$$W_{ка} = \frac{U_{фр}}{4.44 \cdot f_{н} \cdot F_{\delta э} \cdot a_1 \cdot K_{р} \cdot n_{кф} \cdot n_{п} \cdot K_{w}}; \qquad (18)$$

$$X_{а} = 2 \cdot \pi \cdot f_{н} \cdot a_0 \cdot W_{ка}^{2} \cdot n_{кф}, \qquad (19)$$

где $U_{фр}$ – напряжение фазы обмотки якоря расчётное; $F_{\delta э}$ – МДС эквивалентного воздушного зазора (10); a_0, a_1 – постоянная и первая гармоника магнитной проводимости воздушного промежутка под полюсным выступом статора; $K_{р}$ – число полюсных выступов, охватываемых катушкой обмотки якоря; $n_{п}$ – число пакетов статора с обмотками якоря; K_{w} – обмоточный коэффициент; $f_{н}$ – номинальная частота тока якоря, причём

$f_{н} = \frac{Z_r \cdot n_{н}}{60}$ ($n_{н}$ – номинальная частота вращения ротора).

Для трёхфазного (m = 3) генератора с мостовым выпрямителем

$$I_{ан} = \frac{I_{dн}}{\sqrt{3}} = \frac{P_{dн}}{U_{dн} \cdot \sqrt{3}}; \; U_{фр} = \frac{U_{dр}}{\sqrt{2} \cdot \sqrt{3}}; \; K_{v} = \frac{U_{dр}}{U_{dн}} = 1.05 \ldots 1.15, \qquad (20)$$

где $P_{dн}$, $U_{dн}$ – номинальные мощность и напряжение выпрямленного тока генератора; $U_{фр}$, $U_{dр}$ – расчётные фазное и выпрямленное напряжения.

Учитывая выражения для $F_{\delta э}$ (10), $F_{в\delta}$ (16), $W_{ка}$ (18), $I_{ан}$ (20) и рекомендации по выбору значений K_a, $K_в$, K_v, можно для трёхфазного генератора с мостовым выпрямителем определить его воздушный зазор в соответствии с выражением

$$\delta = \frac{\mu_0}{B_{\delta}} \cdot \sqrt{\frac{K_{v} \cdot P_{dн}}{4.44 \cdot \sqrt{3} \cdot K_{а} \cdot K_{в} \cdot n_{\delta} \cdot f_{н} \cdot a_1 \cdot n_{кф} \cdot n_{п} \cdot K_{р} \cdot K_{w}}}. \qquad (21)$$

Для генератора без выпрямителя

$$I_{ан} = \frac{S_{н}}{3 \cdot U_{фн}}; \; K_{и} = \frac{U_{фр}}{U_{фн}} = 1.1 \ldots 1.15, \qquad (22)$$

где $S_н$, $U_{фн}$ – номинальные полная мощность и фазное напряжение генератора, поэтому для них

$$\delta = \frac{\mu_0}{B_\delta} \cdot \sqrt{\frac{\sqrt{3} \cdot K_u \cdot S_н}{4.44 \cdot K_a \cdot K_в \cdot n_\delta \cdot f_н \cdot a_1 \cdot n_{кф} \cdot n_п \cdot K_p \cdot K_w}}, \quad (23)$$

Так, например, для проекта авиационного двухпакетного ($n_п = 2$) аксиального генератора мощностью $S_н = 40$ кВ · А, имеющего $n_н = 8000$ об/мин, $Z_г = 20$, $f_н = 2670$ Гц, $B_\delta = 1.6$ Тл, $n_\delta = 2$, $n_{кф} = 4$, $K_p = 1$, $K_w = 1$, $D = 172$ мм, $l = 50$ мм, выбранные значения $K_a = 0.6$; $K_в = 1.2$; $K_u = 1.1$, воздушный зазор:
а) в соответствии с (23) будет равен $\delta = 0.8$ мм;
б) в соответствии с (17) будет

$$\delta \le 0.02 + \frac{\sqrt{D \cdot l}}{500} = 0.02 + \frac{\sqrt{17.2 \cdot 5}}{500} = 0.39 \text{ см} \approx 0.4 \text{ мм}$$

или находиться в диапазоне

$$\left(\frac{1}{200} \cdots \frac{1}{300}\right) \cdot D = \left(\frac{1}{200} \cdots \frac{1}{300}\right) \cdot 172 = (0.86 \ldots 0.58) \text{ мм.}$$

Литература

[1] Серебряков А. Д. (1999) *Индукторные электрические машины с улучшенными техническими характеристиками*. РАУ, Рига, 108

[2] Серебряков А. Д. (1995) Об эффективности применения индукторных машин в авиации, *Сборник научных трудов РАУ*, Рига, 45–53

[3] Домбур Л. Э. (1984) *Аксиальные индукторные машины.* Зинатне. Рига, 250

Received on the 21st of February 2004

Computer Modelling & New Technologies, 2004, Volume 8, No.1
Transport and Telecommunication Institute, Lomonosov Str.1, Riga, LV-1019, Latvia

Authors' index

Yuri N. Shunin (born March 6, 1951 in Riga)

- Vice-rector on innovation work (Information Systems Institute), professor, Dr.Sc. Habil.
- *Director of specialities*: Semiconductor Electronics & Technologies, Computer simulation of semiconductor technologies (Transport and Telecommunication Institute, Riga)
- *Director of speciality:* Information Systems (Information System Institute)
- **University study**: Moscow physical and technical institute (1968-1974)
- Ph.D. (physics & mathematics) on solid-state physics (1982, Physics Institute of Latvian Academy of Sciences), Dr. Sc. Habil (physics & mathematics) on solid state physics (1992, Ioffe Physical Institute of Russian Academy of Sciences)
- **Publications:** 250 publications, 1 patent
- **Scientific activities**: solid state physics, physics of disordered condensed media, amorphous semiconductors and glassy metals, semiconductor technologies, heavy ion induced excitations in solids, mathematical and computer modelling, system analysis

Igor V. Kabashkin (born in Riga, 1954)

- Vice-rector for Research and Development Affairs of Transport and Telecommunication Institute, Professor, Director of Telematics and Logistics Institute
- PhD in Aviation (1981, Moscow Institute of Civil Aviation Engineering), Dr.Sc.Habil. in Aviation (1992, Riga Aviation University), Member of the International Telecommunication Academy, Member of IEEE, Corresponding Member of Latvian Academy of Sciences (1998)
- **Publications:** 300 scientific papers and 67 patents
- **Research activities:** information technology applications, operations research, electronics and telecommunication, analysis and modelling of complex systems, transport telematics and logistics

Eugene Kotomin (born September 20, 1949, Vilnius, Lithuania)

Professor, Dr. Sc. Habil.**,** Head of Theoretical Laboratory of Institute Solid State Physics , University of Latvia
University study: University of Latvia (Faculty of Physics), 1971
Dr.habil.phys. (in Solid State Physics) (Doctor of Science in former USSR). Title of Thesis: "Theory of Defect Accumulation and Recombination in Ionic Crystals Controlled by Electron Tunnelling", Institute of Physics, Latvian Academy of Sciences, 1988
Publications: 3 books and more than 300 papers
Interests:
Theoretical and Statistical Physics ; Solid State Physics ; Chemical Physics of Condensed Matter; Theory of Defects in Nonmetallic Solids
Head of Project. Physics of Metal/Oxide Interfaces. *Joint project with University College London, UK,* 1998-1999
Head of Project. Large Scale Computer Modelling of Materials. *Joint project with Royal Academy of Sciences, Sweden,* 1999-2000

Vladimir Kuzovkov (born April 13, 1948, Moscow, Russia)

Professor, Dr.Habil.phys, Leading Researcher of University of Latvia,
Institute of Solid State Physics, University of Latvia,
e-mail: kuzovkov@latnet.lv
Interests:
Theoretical and Statistical Physics ; Solid State Physics ; Diffusion-Controlled Reactions in Condensed Matter ; Theory of Surface Catalytic Reactions
Education:
University of Latvia (Faculty of Physics), 1971
Academic and Professional Experience:
Awards:
International Science Foundation (ISF) grant, 1992
International Science Foundation Research Grant. Defects in Oxide Crystals, 1994-1996; NATO Research Grant, 1994; Volkswagen Research Grant (Germany), 1996-1997

Albert Serebryakov (born 1933)

Dr.Sc.Habil.Eng., professor of Department of technical usage of aviation and radio-electronic equipment of Riga Aviation University
Education:
Riga Civil Aviation Engineering Institute, post-graduation – 1964-1966. 1975-1985-Head of Department, 1980-1990 – Dean of Faculty of Aviation Equipment
1997 - professor. Scientific works – 150, patents – 42
Scientific interests:
electric equipment, electroenergetics

Wenbin Luo

Received a B.S. and M.S. degree in Electronics Engineering from Fudan University, Shanghai, China, in 1996 and 1999, respectively. He received the M.S. degree in Statistics and the Ph.D. degree in computer engineering from the University of New Mexico, Albuquerque, New Mexico, in 2002 and 2003, respectively. He is an assistant professor in the Engineering Department at St. Mary's University, San Antonio, Texas. He has published his research papers in the areas of data structures & algorithms and digital image processing. He has served as reviewer for several International Journals and Conferences. He is a member of IEEE.

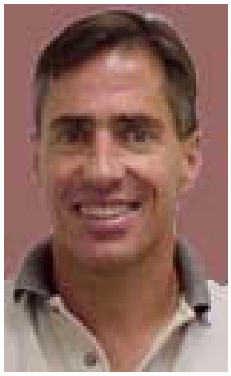

Gregory L. Heileman

Received the BS degree from Wake Forest University in 1982, the MS degree in Biomedical Engineering and Mathematics from the University of North Carolina--Chapel Hill in 1986, and the PhD degree in Computer Engineering from the University of Central Florida in 1989. He is currently a Professor in the Electrical and Computer Engineering Department at the University of New Mexico, Albuquerque, NM. He has published over 80 research papers in International Journals and Conferences, and a book. He is an associate editor for the ACM Journal of Experimental Algorithmics, a senior member of the IEEE Computer Society, a member of the Association for Computing Machinery , and a member of the International Neural Network Society.

Adolfas Baublys, Prof., Habil. Dr, *born September 5, 1941 in Laukininkai, Varena district, Lithuania*

University study: Kaunas Politechnical Institute (1967)
Short description of work experience. Worked as an engineer-technologist in the Vilnius Drill Plant in 1959–1962. During 1962–1980 he worked in the branch office of the Experimental Scientific Research Institute of metal cutting machines as the Head of the Sector and Head of the laboratory. In 1969 he defended a thesis of Doctor of technical sciences; in 1978 – Habil. Dr. thesis. In 1980–1997 he was the Head-Professor of the Transport Management Department at the Vilnius Gediminas Technical University. Since 4 May 1997 – Director of the Transport Science Institute.
Field of Scientific Research. Transport policy; Strategy of Transport System Development, Modelling and Forecasting. *Monographs:* „Cargo Transportation by Railway, Water and Air Transport“ (1995); „Introduction to Transport System Theory“ (1997); „Cargo Transportation“ (1998). *Textbooks:* „Passenger and Cargo Transportation by Road Transport“ (1994, 1995); „Transport System“ (1995, 1996); „Transport Policy“ (1996); „International Transportation by Road Transport“ (1996). He is the author of 210 scientific articles. Twenty doctor's theses were defended under his guidance.
Social-organisational activities. In 1991 he was elected a member-expert of the Lithuanian Science Academy. He is also the Chairman of the Commission on Transport Technology for science at the Vilnius Gediminas Technical University; Chief and Scientific Editor of „Transport“, the prestige journal of Lithuania.
Office address: Vilnius Gediminas Technical University, Transport Research Institute, Plytines 27, LT-2040 Vilnius, Lithuania, ph: 370 2 31 56 13; fax: 370-2 31 56 13, e-mail: abaublys@takas.lt

CUMULATIVE INDEX

COMPUTER MODELLING and NEW TECHNOLOGIES, volume 8, No. 1, 2004

(Abstracts)

V. N. Kuzovkov, E. A. Kotomin, G. Zvejnieks. Modelling of Pattern Formation in Thin Metallic Film Growth on Crystalline Substrates, *Computer Modelling and New Technologies,* vol. 8, No.1, 2004, pp. 7–19.

We present and discuss results of the kinetic MC simulations of the pattern formation during the adsorption of mobile metal atoms on crystalline substrate. Simulations are based on a new complete axiomatic approach to the kinetics of diffusion-controlled processes with energetic interactions (the *standard model* described in Appendix A). Pattern formation simulated for submonolayer metal coverage is characterized in terms of the joint correlation functions for spatial distribution of adsorbed atoms. We demonstrate that the patterns obtained are defined by the ratio of the atom mutual attraction energy to the substrate temperature. Kinetic MC simulations confirm the distinctive average distance between two-dimensional metal islands, estimated by means of scaling approach.

Keywords: *pattern formation, thin films, MC simulations*

I. B. Frenkel. Nonlinear Problem of a Thermal Conductivity in a Solid Cylinder, *Computer Modelling and New Technologies,* vol. 8, No.1, 2004, pp. 20–23.

Method of perturbations [2], [4] can be applied with great success to the solution of the boundary-value problems of thermal conductivity, solved by an integration of the nonlinear differential equations. In the paper we propose the combination of the small parameter method and method of perturbations for solution of a nonlinear problem of a thermal conductivity in the cylinder under condition of a linear dependence of thermal conductivity factors and a thermal capacitance on temperature.

Keywords*: thermal conductivity, heat conduction equation, mathematical methods*

A. Baublys. Mathematical Models with Application of Statistical Information in Transportation Management Process, *Computer Modelling and New Technologies,* vol. 8, No.1, 2004, pp. 24–38.

In the course of freight transportation its technological process is influenced by lots of random factors. Classification of random factors in the whole hierarchical structure of the technological transportation process is presented, together with the assessment of the dependence of separate random factors. Statistical information on freight and transport flows is renewed and replenished in the course of time. With the growth of information amounts the costs of its storage increase as well. Therefore the relevant algorithms for obtaining required statistical assessments with the least statistical information are presented in the article. It is deduced that in the modelling of transport networks and freights as well as the flows of transport means in them, it is analytically proper to describe random factors by the non-parametric assessment.

Keywords: *freight transportation, mathematical modelling*

W. Luo, G. L. Heileman. A Fast and Robust Watermarking Method for JPEG Images, *Computer Modelling and New Technologies,* vol. 8, No.1, 2004, pp. 39–47.

In this paper, a JPEG domain image watermarking method that utilizes spatial masking is presented. The watermarking algorithm works in the compressed domain, and can be implemented efficiently in real-time (only 50ms is required for a 512x512 24-bit color image on a 700MHz computer). In many applications, particularly those associated with delivering images over the Internet, the ability to watermark images in real-time is required. In order to achieve a real-time watermarking capability, the proposed technique avoids many of the computation steps associated with JPEG compression. Specifically, the forward and inverse DCT do not need to be calculated, nor do any of the computations associated with quantization. Robustness to JPEG compression, different kinds of noise (additive, salt & pepper, and speckle) and image cropping attacks are achieved with the proposed system, and the relationship between watermark robustness and watermark position is described. A further advantage of the proposed method is that it allows a watermark to be detected in an image without referencing to the original unwatermarked image, or to any other information used in the watermark embedding process.

Keywords: *image watermarking, spatial masking*

A. D. Serebryakov. Calculation Peculiarities of Aviation Inductor Generators, *Computer Modelling and New Technologies,* vol. 8, No.1, 2004, pp. 48–52. (in Russian)

Analytical expression for definition of the air-gap of the axial inductor generator is obtained. The procedure of the account of reaction of an anchor is considered.

Keywords: *inductor generator, anchor reaction, air-gap*

V. N. Kuzovkovs, E. A. Kotomin, G. Zvejnieks. Modeļa izveides modelēšana, pieaugot plānajai metāliskajai kārtai kristāliskajā substrātā, *Computer Modelling and New Technologies,* 8.sēj., Nr.1, 2004, 7.–19. lpp.

Raksta autori izskata kinētisko *MC* simulāciju rezultātus, resp. metāla atomu adsorbcijas laikā, kuri pārvietojas kristāliskajā substrātā, radušos modeli. Simulācijas bāzējas uz pilnīgi jaunas pabeigtas aksiomātiskas pieejas difūzi-kontrolējamo procesu kinētikai ar enerģiskām savstarpējām iedarbībām (standarta modelis ir aprakstīts Pielikumā A).

Atslēgvārdi: modeļa veidošana, plānās kārtas, *MC* simulācijas

I. B. Frenkel. Siltumvadītspēja cietajā cilindrā nelineāra problēma, *Computer Modelling and New Technologies,* 8.sēj., Nr.1, 2004, 20.–23. lpp.

Rakstā autori piedāvā mazā parametra metodes kombināciju un perturbāciju metodi, lai risinātu siltumvadāmības nelineāru problēmu cilindrā, tādos apstākļos, kad siltumvadāmības faktori ir lineārā atkarībā, un termiskā kapacitāte ir atkarīga no temperatūras.

Atslēgvārdi: siltumvadītspēja, karstuma vadītspējas vienādojums, matemātiskās metodes

A. Baublys. Transportēšanas vadīšanas procesa matemātiskie modeļi, pielietojot statistisko informāciju, *Computer Modelling and New Technologies,* 8.sēj., Nr.1, 2004, 24.–38. lpp.

Daudz nejaušu faktoru ietekmē kravu transportēšanu un to tehnoloģisko procesu.

Rakstā tiek izklāstīta nejaušu faktoru klasifikācija visa tehnoloģiskā procesa hierarhiskajā struktūrā kopā ar atkarības no atsevišķiem nejaušiem faktoriem izvērtēšanu.

Atslēgvārdi: kravu transportēšana, matemātiskā modelēšana

W. Luo, G. L. Heileman. Ātra un robusta ūdens zīmēšanas metode *JPEG* attēliem, *Computer Modelling and New Technologies,* 8.sēj., Nr.1, 2004, 39.–47. lpp.

Šajā rakstā tiek izskatīta *JPEG* domēna attēla ūdens zīmēšanas metode, kur tiek pielietota telpiska maskēšana.

Ūdens zīmēšanas algoritms tiek izmantots saspiestā domēnā, un var būt efektīvi pielietots reālā laikā (tikai 50ms ir nepieciešami 512x512 24-bitu krāsu attēlam 700 MHz datoram).

Atslēgvārdi: attēlu ūdenszīmju veidošana, telpiska maskēšana

A. D. Serebryakov. Aviācijas induktora ģeneratora aprēķina, *Computer Modelling and New Technologies,* 8.sēj., Nr.1, 2004, 48.–52. lpp.

Rakstā ir izklāstīta aksiālā induktora ģeneratora gaisa-starpas analītiska definīcija. Enkura reakcija tiek ņemta vērā, izstrādājot doto metodiku.

Atslēgvārdi: induktora ģenerators, enkura reakcija, gaisa-starpa

COMPUTER MODELLING & NEW TECHNOLOGIES

ISSN 1407-5806 & ISSN 1407-5814(on-line)

THE JOURNAL IS DESIGNED FOR PUBLISHING PAPERS CONCERNING THE FOLLOWING FIELDS OF RESEARCH:

- mathematical and computer modelling
- mathematical methods in natural and engineering sciences
- physical and technical sciences
- computer sciences and technologies
- semiconductor electronics and semiconductor technologies
- aviation and aerospace technologies
- electronics and telecommunication
- navigation and radar systems
- telematics and information technologies
- transport and logistics
- economics and management
- social sciences

Articles can be presented in journal in English (preferably), Russian, German and Latvian (at the option of authors). All articles are reviewed.

EDITORIAL CORRESPONDENCE

Transporta un sakaru institūts (Transport and Telecommunication Institute)
Lomonosova iela 1, LV-1019, Riga, Latvia. Phone: (+371)-7100593. Fax: (+371)-7100535
E-mail: journal@tsi.lv, http:// www.tsi.lv

COMPUTER MODELLING AND NEW TECHNOLOGIES, 2004, Vol. 8, No.1
Scientific and research journal of Transport and Telecommunication Institute (Riga, Latvia)
The journal is being published since 1996.

The Camera-Ready Copies

PREPARATION OF CAMERA-READY TYPESCRIPT: COMPUTER MODELLING AND NEW TECHNOLOGIES

A Guide for Authors

A.N. AUTHOR
Affiliation
Institute address

Abstract reviews the main results and peculiarities of a contribution. Abstract is presented always in English or in English and the second (presentation) language both.
Keywords: main terms, concepts

1. Introduction

These instructions are intended to provide guidance to authors when preparing camera-ready submissions to a volume in the **CM&NT**. Please read these general instructions carefully before beginning the final preparation of your camera-ready typescript.

Two ways of preparing camera-ready copy are possible:
(a) preparation on a computer using a word processing package;
(b) printed copy fitted for scanning.

2. Printer Quality, Typing Area and Fonts

IMPORTANT:

If you produce your camera-ready copy using a laser printer, use a 15 x 23 cm typing area (in A4 format: 30 mm – left, 30 mm – right, 30 mm – top, 30 – bottom, line spacing – single), as in these instructions, in combination with the **10 points Times** font. The pages will then be reproduced one to one in printing.

Fonts

The names and sizes of fonts are often not the same on every computer system. In these instructions the Times font in the sizes 10 points for the text and 8 points for tables and figure legends are used. The references section should be in the 10 points font.

3. Format and Style

The text should be in clear, concise English (or other declared language). Please be consistent in punctuation, abbreviations, spelling (***British English***), headings and the style of referencing.

Camera-ready copy will be printed exactly as it has been submitted, so please make sure that the text is proofread with care.

In general, if you prepare your typescript on a computer using a word processing package, use styles for the font(s), margin settings, headings, etc., rather than inserting these layout codes every time they are needed. This way, you will obtain maximum consistency in layout. Changes in the layout can be made by changing relevant style(s).

4. Layout of the Opening Page

A sample for the opening page of a contribution is shown in Figure 1 on page 3.
Requirements for the opening page of a contribution are (see also Figure 1): the titles should always be a centered page and should consist of: the title in capital letters, bold font, flush center, on the fourth text line; followed by the subtitle (if present) in italics, flush center, with one line of white above. The author's name(s) in capitals and the affiliation in italics should be centered and should have two lines of white space above and three below, followed by the opening text, the first heading or the abstract.

5. Headings

Please distinguish the following four levels of headings:

1. First-order Heading

This heading is in bold, upper and lowercase letters, numbered in Arabic figures, and has two lines of space above and one line below. The text begins full out at the left margin.

1.1. SECOND-ORDER HEADING IN CAPITALS

This heading is in roman capitals, numbered in Arabic figures and has one line of space above and below. The text begins full out at the left margin.

1.1.1. *Third-order Heading in Italics*

This heading is in italics, upper and lower case letters, numbered in Arabic figures and has one line of space above and no space below. The text begins full out at the left margin.

Fourth-order Heading in Italics. This heading is in italics, upper and lowercase letters, with one line of space above the heading. The heading has a full stop at the end and the text runs on the same line.

↕ 3 blank lines

TITLE OF CONTRIBUTION

Subtitle of Contribution

↕ 2 blank lines

A.N. AUTHOR

Affiliation

Institute address

↕ 3 blank lines

Abstract

↕ 2 blank lines

First text line

Figure l. Example of an opening part of contribution to a Volume of CM&NT

6. Figures and Photographs

- *Line drawings* must be submitted in original form, on good quality tracing paper, or as a glossy photographic print.
- *Halftone photographs* must be supplied as glossy prints.
- *Colour illustrations.* Colour illustrations are more expensive and the author is expected to cover the extra costs. Please consult with Editors about this.

Mount all illustrations directly into the text at the appropriate places. Alternatively, it is acceptable to leave the appropriate space blank in the text, and submit the illustrations separately. In this case You must put the figure numbers in pencil in the open spaces in the text and on the back of the figures. Also indicate the top of the illustration.

For computer plotting the ORIGIN Software is preferable.

- Legends for figures/illustrations should not be incorporated in the figure itself and they should be listed in numerical order (headed as "*Figure 1.*", "*Figure 2.*" etc.). The legends should be set centered, below the figure.

7. Displayed Equations

Displayed equations should be in the left side of the page, with the equation number in parentheses, flush right.

$$E_{int} = \iint \psi^{+}(\mathbf{x})\psi(\mathbf{x})K(\mathbf{x}-\mathbf{x}')(-div\mathbf{P}(\mathbf{x}'))d^3xd^3x', \quad (1)$$

$$K(\mathbf{x}-\mathbf{x}') = C_0 \frac{exp(-\lambda(|\mathbf{x}-\mathbf{x}'|)}{|\mathbf{x}-\mathbf{x}'|}. \quad (2)$$

Font sizes for equations are: 12pt – full, 7pt – subscripts/superscripts, 5pt – sub-subscripts/superscripts, 18pt – symbols, 12pt – subsymbols.

8. Tables

Please center tables on the page, unless it is necessary to use the full page width. Exceptionally large tables may be placed landscape (90^0 rotated) on the page, with the top of the table at the left-hand margin. An example of a table is given below:

TABLE 1. National programs of fusion research [1]

Experiment	Type	Laboratory	Task	Begin of operation
JET	tokamak	Joint European Torus, Culham, UK	Plasma physics studies in the region close to ignition	1983
TEXTOR	tokamak	FA, Jülich. Germany	Studies of plasma-wall interaction	1982
TORE SUPRA	tokamak	CEA, Cadarache, France	Testing of super-conducting coils, stationary operation	1988
ASDEX Upgrade	tokamak	IPP, Garching, Germany	Plasma boundary studies in divertor plasmas	1990
WENDELSTEIN 7-AS	stellarator	IPP, Garching, Germany	Testing the principles of "advanced stellarator"	1988
WENDELSTEIN 7-X	stellarator	IPP, Greifswald, Germany	Testing feasibility of "advanced stellarator" for power station	2004

9. References

The References should be typeset in a separate section as a numbered list at the end of your contribution in the following style:

Journal articles should consist of as follows: author's name, initials, year, title of article, journal title, volume number, inclusive page numbers, e.g.:

[1] Dumbrajs O. (1998) Nuclear Fusion. *RAU Scientific Reports & Computer Modelling & New Technologies* **2***,* aa-zz
[2] Kiv A.E., Polozovskaya I.A., Tavalika L.D. and Holmes S. (1998) Some problems of operator-machine interaction. *RAU Scientific Reports & Computer Modelling & New Technologies* **2***,* aa-zz
[3] Shunin Yu.N. (1996) Elementary excitations and radiation defects in solids induced by swift heavy ions. *RAU Scientific Reports & Solid State Electronics & Technologies* **1**, 15-35
[4] Schwartz K. (1996) Excitons and radiation damage in alkali halides. *RAU Scientific Reports & Solid State & Electronics & Technologies* **1**, 3-14

Book references should consist of as follows: author's name, initials, year, title of book, publisher, place of publication, e.g.:

[5] Schwartz K. (1993) The Physics of Optical Recording. Springer-Verlag, Berlin Heidelberg New York

[6] Shunin Yu.N. and Schwartz K.K. (1997) Correlation between electronic structure and atomic configurations in disordered solids. In: R.C. Tennyson and A.E. Kiv (eds.). Computer Modelling of Electronic and Atomic Processes in Solids. Kluwer Academic Publishers, Dordrecht, pp. 241-257 .

Unpublished papers should consist of as follows: author's name, initials, year (or: in press), title of paper, report, thesis, etc., other relevant details, e.g.:

[7] Shunin Yu.N. (1995) Elementary Excitations in amorphous solids accompanying the swift heavy ions passages. Private communication. GSI Seminar. Darmstadt

The references above should be cross-referenced by numbers within square brackets:
...as cited in [1], or Kiv *et al.* [2]... The use of author's initials for cross-references is not encouraged.

10. Authors Index

Editors form the author's index of a whole Volume. Thus, all contributors are expected to present personal colour photos with the short information on the education, scientific titles and activities.

11. Submission

Check your typescript very carefully before it is submitted. Submit two copies of the typescript to the Editors of the Volume. Always retain a copy of all material submitted as backup.

11.1. DISK FORMATS AND WORD PROCESSING PACKAGES

If you want to present contributions electronically please before submitting accord with the Editors the details on your computer system, your word processing package and version (MS Word 6 and above versions are preferable) and the way of transfer on the information (disk or Internet).

Acknowledgements

Acknowledgements (if present) mention some specialists, grants and foundations connected with the presented paper. The first page of the contribution should start on page 1 (right-hand, upper, without computer page numbering). Please paginate the contributions, in the order in which they are to be published. Use simple pencil only.

NATURE AND COMPUTER WORLD
Scientific popular journal

ПРИРОДА И КОМПЬЮТЕРНЫЙ МИР
Научно-популярный журнал

DABA UN DATORPASAULE
Zinātniski populārais žurnāls

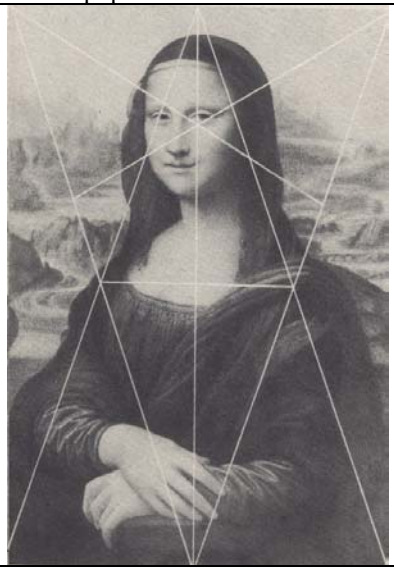

PUBLISHERS:
TRANSPORT AND TELECOMMUNICATION INSTITUTE
***TRANSPORTA UN SAKARU INSTITŪTS** (TSI)*
&
INFORMATION SYSTEMS INSTITUTE
***INFORMĀCIJAS SISTĒMU AUGSTSKOLA** (ISMA)*

NATURE AND COMPUTER WORLD,
PUBLISHED SINCE 2001
ISSN 1407-8422
ISSN 1407-8422 **- on-line**

Editorial office:
Nature and Computer World,
Lomonosov 1, Build. 4, LV-1019, Riga, Latvia
shunin@tsi.lv, kiv@tsi.lv

N&CW is the new scientific popular journal addressed to senior school students. It pays attention to some actual fields of undergraduate studies:

- Mathematics
- Physics
- Computers
- Programming and Computer Modelling
- Nature Phenomena

We are open for collaboration in these directions in the framework of N&CW and ready to consider corresponding materials. All articles are reviewed.